# SOL-GEL SYNTHESIS OF ANTIBACTERIAL SILVER-DOPED SILICA POWDERS FROM SODIUM SILICATE (WATER GLASS)

A THESIS SUBMITTED TO
THE GRADUATE SCHOOL OF NATURAL AND APPLIED SCIENCES
OF
MIDDLE EAST TECHNICAL UNIVERSITY

BY

EVRİM ÖZDEM TUFAN

IN PARTIAL FULFILLMENT OF THE REQUIREMENTS
FOR
THE DEGREE OF MASTER OF SCIENCE
IN
METALLURGICAL AND MATERIALS ENGINEERING

JUNE 2013

Approval of the thesis:

**SOL-GEL SYNTHESIS OF ANTIBACTERIAL SILVER-DOPED SILICA POWDERS FROM SODIUM SILICATE (WATER GLASS)**

Submitted by **EVRİM ÖZDEM TUFAN** in partial fulfillment of the requirements for the degree of **Master of Science in Metallurgical and Materials Engineering Department, Middle East Technical University** by,

Prof. Dr. Canan Özgen _____
Dean, **Graduate School of Natural and Applied Sciences**

Prof. Dr. Hakan Gür _____
Head of Department, **Metallurgical and Materials Engineering**

Assoc. Prof. Dr. Caner Durucan _____
Supervisor, **Metallurgical and Materials Engineering Dept., METU**

**Examining Committee Members:**

Prof. Dr. M. Vedat Akdeniz _____
Metallurgical and Materials Engineering Dept., METU

Assoc. Prof. Dr. Caner Durucan _____
Metallurgical and Materials Engineering Dept., METU

Assoc. Prof. Dr. Arcan Dericioğlu _____
Metallurgical and Materials Engineering Dept., METU

Assoc. Prof. Dr. H. Emrah Ünalan _____
Metallurgical and Materials Engineering Dept., METU

Assist. Prof. Dr. Emren Nalbant Esentürk _____
Chemistry Dept., METU

**Date:** 10 June 2013

**I hereby declare that all information in this document has been obtained and presented accordance with the academic rules and ethical conduct. I also declare that, as required by these rules and conduct, I have fully cited and referenced all material and results that are not original to this work.**

Name, Last name: Evrim Özdem TUFAN

Signature: :

## ABSTRACT

SOL-GEL SYNTHESIS OF
ANTIBACTERIAL SILVER-DOPED SILICA POWDERS
FROM SODIUM SILICATE (WATER GLASS)

Tufan, Evrim Özdem
M.Sc., Department of Metallurgical and Materials Engineering
Supervisor: Assoc. Prof. Dr. Caner Durucan

June 2013, 49 pages

Sol-gel processing routes for the synthesis of antibacterial silver-doped silica (Ag-$SiO_2$) powders from an inorganic precursor, sodium silicate ($Na_2SiO_3$, water glass), have been established. For the synthesis of $SiO_2$ powders, two different processing approaches were used. In the first one (indirect synthesis), silver ions were incorporated into the immature wet silica gels obtained from sodium silicate by the exposure of the silica gels to aqueous silver nitrate ($AgNO_3$) solutions. In the second one, silver was directly incorporated into the aqueous silica forming formulations during sol development. In the initial work, the effect of washing treatment on the sodium removal from the silicate by-products has been investigated for the indirect synthesis route. Then, for both routes, silver-doped silica (Ag-$SiO_2$) powders were synthesized based on the results of washing treatment studies. The effect of silver incorporation amount on the silver formation efficiency during thermal maturing of silica network (200-800°C) was examined. The phase analysis of the powders was performed using x-ray diffraction (XRD). The antibacterial activity of the powders was determined against *Staphylococcus aureus* and *Escherichia coli* by disk diffusion method. Furthermore, the effect of synthesis route, the silver dopant amount ($[AgNO_3]/[Na_2SiO_3]$ ratio) and the calcination temperature on the structural properties and on the antibacterial activity of the powders were investigated. The time-dependent antibacterial performance was evaluated for the samples obtained from different processing routes and parameters. The investigations revealed that the silver-doped silica powders were much more effective against *Staphylococcus aureus* than *Escherichia coli*. In addition, a high level of antibacterial activity was observed especially for the powders obtained by indirect synthesis route with low silver dopant amount.



**Keywords:** Silver-doped, antibacterial, sodium silicate, sol-gel method, silica matrix

# ÖZ


SOL-JEL YÖNTEMİYLE
SODYUM SİLİKAT (CAM SUYU) KULLANARAK
ANTİBAKTERİYEL GÜMÜŞ AŞILANMIŞ SİLİKA TOZLARININ SENTEZİ

Tufan, Evrim Özdem
Yüksek Lisans, Metalurji ve Malzeme Mühendisliği Bölümü
Tez Yöneticisi: Doç. Dr. Caner Durucan

Haziran 2013, 49 sayfa

İnorganik başlangıç kimyasalı olan sodyum silikat ($Na_2SiO_3$, cam suyu) kullanılarak, sol-jel tekniği ile antibakteriyel özellik gösteren gümüş aşılanmış silika (Ag-$SiO_2$) tozları geliştirmek için sentez yöntemleri belirlendi. $SiO_2$ tozlarının sentezlenmesinde iki farklı proses yaklaşımı kullanıldı. Bunlardan ilkinde (dolaylı sentez), sodyum silikattan elde edilmiş ve olgunlaşmamış yaş silika jellerin sulu gümüş nitrat ($AgNO_3$) çözeltisine maruz bırakılmasıyla gümüş iyonları sisteme aşılandı. İkinci sentezleme yönteminde ise, gümüş içeren sıvı çözeltiler direk olarak silika oluşturan sıvı sol formulasyonlarına eklenerek gümüş aşılaması gerçekleştirildi. Öncelikle, dolaylı sentez yolu için, sodyumun silikat yan ürünlerinden uzaklaştırılması için yıkama işleminin etkisi çalışıldı. Sonrasında, her iki sentezleme yolu için, yıkama çalışmasının sonuçları esas alınarak gümüş aşılanmış silika tozları (Ag-$SiO_2$) sentezlendi. Aşılanan gümüş miktarının, silika matriksin ısıl olgunlaşması sırasında (200-800°C) gümüş oluşum verimine etkisi incelendi. Tozların faz analizi x-ışını kırınımı (XRD) ile gerçekleştirildi. Gümüş aşılanmış silika (Ag-$SiO_2$) tozlarının *Staphylococcus aureus* ve *Escherichia coli* bakterilerine karşı gösterdiği antibakteriyel performans, disk difüzyon metodu ile belirlendi. Sentezleme yöntemi, aşılanan gümüş miktarı ($[AgNO_3]/[Na_2SiO_3]$ oranı) ve kalsinasyon sıcaklığının, tozların yapısal ve antibakteriyel özelliklerine olan etkisi araştırıldı. Tozların *Staphylococcus aureus* ve *Escherichia coli* bakterilerine karşı olan antibakteriyel aktivitenin zamana bağlı değişimi incelendi. Elde edilen sonuçlar, gümüş aşılanmış tozların *Staphylococcus aureus* bakterisine karşı daha fazla etkili olduğunu gösterdi. Ayrıca, gümüşün silika matrikse dolaylı sentez yolu ile aşılandığı düşük gümüş miktarlı tozların daha yüksek antibakteriyel özellik gösterdiği belirlendi.



**Anahtar Kelimeler:** gümüş aşılanmış, antibakteriyel, sodyum silikat, sol-jel methodu, silika matriks

***To my parents …***

**ACKNOWLEDGEMENTS**

First of all, I would like to express my special thanks to Assoc. Prof. Dr. Caner Durucan for his continuous guidance, support, motivation and encouragement during this study. I sincerely appreciate the time and effort he have spent to improve my experience during my thesis.

Further, I would like to thank to all the staff members in the metallurgical and materials engineering department for their support and help throughout this study. I deeply thank to special lab-mates Özlem Altıntaş Yıldırım, Onur Rauf Bingöl, Tümerkan Kesim, Hakan Yavaş, Gözde Alkan and especially to Betül Akköprü Akgün for their helpful discussions and support during my experiments. She has always been more than a lab-mate for me. I also would like to thank my friends Mine Kalkancı and Saeid Pournaderi.

I especially thank to Necmi Avcı, Saffet Ayık, Gözde Alkan, Özlem Altıntaş Yıldırım, Tümerkan Kesim, Onur Rauf Bingöl, Metehan Erdoğan and Can Yıldırım for their helps in XRD analyses. I also thank to Yusuf Yıldırım for his help in heat treatment studies. Moreover, I would like to thank Nusret Taheri and Osman Aytuzlar of METU Medical Center for their help in antibacterial tests.

I owe my deepest thanks to my mother and my father for their love and patience they have shown throughout my life.

Finally, I would like to thank everybody who was important to the successful realization of the thesis, as well as expressing my apology that I could not mention personally one by one.

**TABLE OF CONTENTS**

## LIST OF TABLES

**TABLES**

## LIST OF FIGURES

**FIGURES**

# CHAPTER 1

# INTRODUCTION

## 1.1 Background information and literature review

### 1.1.1 Antibacterial materials

There is a growing interest in developing materials and surfaces for protection against infectious microorganisms such as bacteria due to the increasing public health concerns. Ideal antibacterial materials should maintain antibacterial property through the service time. Moreover, they should be non-toxic and biocompatible with human cells. They should also not change physical properties (such as color, texture) of the surfaces that they have been applied. Resistance to environmental conditions (light, heat, humidity, etc.) and chemical durability are other important properties that antibacterial materials should possess. Antibacterial materials can be divided into three main groups.

#### 1.1.1.1 Antibacterial materials minimizing the physical contact of bacteria with surfaces

Antibacterial materials in this group minimize physical contact of bacteria with surfaces and as a result of this bacteria is repelled (Tiller et al. 2005). Hydrogel-forming non-charged coatings such as poly(ethylene glycol) films modified with poly(ethylene oxide) can be used to repel bacteria (Desai et al. 1992). Desai et al. 1992 investigated the antibacterial performance of polyethylene films on implant surfaces against various bacteria including *Staphylococcus Epidermis, Staphylococcus Aureus* and *Pseudomonas Aeruginosa*. They found that surface modification achieved by poly(ethylene oxide) significantly decreased the infections during implant usage. Making the material surface ultra hydrophobic (contact angle greater than 150°) is another alternative approach in minimizing the physical contact of bacteria and repelling bacteria (Kurosaka et al. 2000). These surfaces, however, do not terminate bacteria completely. They have bacteriostatic character only inhibiting reproduction of bacteria. They also suffer from poor instability against environmental factors during long-term service. Therefore, they find restricted application fields.

#### 1.1.1.2 Antibacterial materials destroying bacteria on contact

Antibacterial materials in this system are capable of killing bacteria on contact (Tiller et al. 2001, 2005). Coatings of specially synthesized polymers such as poly(4-vinyl pyridine) can be given as an example to this type of antibacterial materials (Tiller et al. 2001). These long stiff hydrocarbon chains acting as molecular knives simply destroy the cell wall by physical contact. In their study, Tiller et al. 2001 attached poly(4-vinyl-N-alkyl pyridinium bromide)

to glass slides. Although these glass surfaces are effective on killing airborne bacteria, on the surfaces other than glass such as ceramics, plastics, metals and wood, it is seen that the number of viable bacterial cells does not decrease due to structural deformations of the polymer knives (Tiller et al. 2001).

Another material to be added to this group is coatings based on photocatalytic $TiO_2$ in which bacteria is killed by light-induced production of hydroxyl radicals (Ohko et al. 2001). As it is known, organic remainders are broken into pieces when titanium dioxide particles are exposed to UV-light. By this method, self-cleaning systems on the outer surfaces of glass, mirror and buildings can be obtained. At the same time, with the addition of silver to titanium dioxide particles, increase in antibacterial property was observed (Page et al. 2007).

#### 1.1.1.3 Antibacterial materials including active biocides

These kind of materials release active biocides and sustain the antibacterial property for a long term. These biocide releasing systems can be divided into five groups: antibiotic, chlorine, iodine, chitosan and metal ion [Pai et al. 2001; Adams et al. 1999; Gottardi 1983; Chen et al. 2005; Jeon et al. 2003]. Biocides destroy wall of the cell and causes change in enzymatic activities which controls nutrition and respiration of bacteria cells. However, these materials are somewhat potentially problematic due to the incompability of the active biocides with the human tissues and environmental concerns related to them. In some cases, bacteria can also develop a natural immune response against the biocide (as observed for antibiotics) and therefore, weaken the overall antibacterial effect (Pai et al. 2001). However, ion-releasing materials, such as silver-containing antibacterial materials do not exhibit most of the negative concerns stated above. Silver is a good candidate for antibacterial material because:

- It is not toxic, caustic or corrosive,
- It has a broad-spectrum biocidal activity,
- It continues to be highly biocidal long after its application to the surface,
- It is cost competitive with several classes of existing antimicrobial compounds,
- It does not foster the development of resistant organisms,
- It is biocompatible with human cells.

In this study, synthesis of sodium silicate based silver-doped antibacterial powders have been investigated. In fact, silver ion has been known as disinfectant and antibacterial material from ancient times. It has been used for water storage. Also, it is known that silver has been used in the treatment of open wound and bone [Grier, 1983].

### 1.1.2 Antibacterial mechanism of silver

Feng et al. 2000 investigated the mechanism of inhibition of silver ions on microorganisms. According to their study, one possible mechanism is that the state of DNA molecules changes from relaxed to condensed which results in the loss of replicating ability. Another possible mechanism is that silver ions interact with sulphydryl (—SH) groups present on the bacteria cell wall, which is a molecular catalyst for many protein/enzymatic activity of the bacteria and therefore inactivates all the natural activity of bacteria (Feng et al. 2000). Figure 1.1 is a schematic of antibacterial mechanism of silver. Bacteria cell walls contain sulphydryl (—SH) groups which are responsible for the basic biological functions of the bacteria. $Ag^{+}$ can react with these groups and form ($S—Ag^{+}$) complex. Once this complex is formed, termination of bacteria occurs as the bacteria can no longer perform enzyme activities which provides cellular nutrition, respiration and multiplication of bacteria.

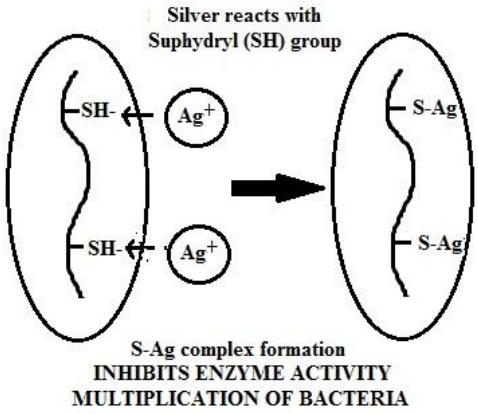


**Figure 1.1** Schematic of antibacterial mechanism of silver.

### 1.1.3 Selection of material for silver-doped materials

There is an increasing demand for silver-doped materials since silver ions show antibacterial property even at low concentrations in the ppb range. It is also known that silver is non toxic which makes the use of silver in commercial products possible since ancient times (Nishino et al. 1996; Ohtani 1997). Although there are antibacterial agents based on organic materials, they cannot be used under conditions where the chemical durability is required. Therefore, antibacterial silver-doped materials based on inorganic materials such as zeolites, calcium phosphate, silica gel, etc. have been developed (Yoshinari and Uchida 1993; Nishino et al. 1996; Ohtani 1997). Silver-doped zeolites show high antibacterial activity and high chemical durability. However, they have low mechanical strength. So, in this study, silica matrix is used in order to synthesize silver-doped materials owing to its chemical and structural durability.

### 1.1.4 Production methods for silver-doped silica materials

#### 1.1.4.1 Sputtering

Sputtering is a vacuum-based evaporation method which literally removes portions of a material called the target, and deposits a thin film/coating onto a flat surface, substrate. The process occurs by bombarding the surface of the target with gaseous ions accelerated by high voltage. When these ions collide with the target, atoms or molecules of the target material are ejected against the substrate. The resulting material is held firmly to the surface by mechanical forces. Although alloy or chemical bond may result in some cases. Sputtering is a successful method for a variety of substrates with electrically conductive or non-conductive materials.

#### 1.1.4.2 Ion implantation

Ion implantation is another vacuum technique which can be used to introduce controlled amounts of foreign atoms into a surface. Ion implantation is a widely used method in materials science research. The ions change the elemental composition of the target. They also result in much chemical and physical change in the target by transferring their energy and momentum to the electrons.

#### 1.1.4.3 Sol-gel method

In order to dope silver into silica, sol-gel method is preferred owing to its advantages. First of all, it is a room temperature and atmospheric pressure process. Moreover, high purity products with good homogeneity in different forms (e.g. film, powder) can be obtained. Furthermore, sol-gel method allows doping various substances to sol-gel derived silica matrices via their impregnation in solutions/suspensions including the dopant. Another advantage of sol-gel method is that the products are porous and the porosity can be controlled. Besides, sol-gel method is inexpensive as it does not require any sophisticated technical instruments (Brinker and Scherer 1990).

##### 1.1.4.3.1 Conventional sol-gel method

Conventional sol-gel technique is based on the hydrolysis of liquid precursors and the formation of colloidal sols. Conventionally, organosilicates [e.g. tetraethyl orthosilicate, $Si(OC_2H_5)_4$, TEOS] are used as precursors in sol-gel method together with water and ethanol. During the process, hydrolysis and condensation reactions of organometallic compounds occur in alcoholic solutions. Chemical reactions during gel formation in conventional sol-gel method is shown in Figure 1.2.

#### 1.1.4.3.2 Alternative sol-gel method

In the present study, sodium silicate precursor ($Na_2SiO_3$) also known as water glass is used instead of metal alkoxide precursor. As sodium silicate ($Na_2SiO_3$) is an inorganic precursor, it is environment friendly. Moreover, it is much cheaper than organic precursor (TEOS). Figure 1.3 illustrates the sol-gel transformation of sodium silicate to silica gel.

### 1.1.5 Silver-doped sol-gel derived silica materials

Silver particles can be doped into silica matrix by dissolving silver nitrate solution in the silica sol. Then silver ions are reduced to metallic silver particles by thermal treatment in air, in an hydrogen atmosphere, by irradiation with UV light or gamma rays (Zayat et al. 1997). Sakka and Kozuka 1998 also studied formation of metal particles from metal ions and states that this can be by one of the following treatments:

(1) Reduction of metal ions by heating the gel in air,
(2) Reduction of metal ions by exposing the gel to UV light,
(3) Reduction of precipitated metal oxide particles by heating in a reducing gas.

Silver-doped silica by sol-gel method can be both in powder or coating form (Weiping and Lide 1996; Wu et al. 2000; Garnica-Romo et al. 2002; Ortega-Zarzosa et al. 2003; Mennig et al. 1997; Zayat et al. 1997; Garnica-Romo et al. 2002; Serezhkina et al. 2003).

#### 1.1.5.1 Silver-doped silica powders processed using organic precursor (TEOS)

Ortega-Zarzosa et al. investigated calcination behavior of silica gel powders modified with silver during heat treatments in air (Ortega-Zarzosa et al., 2003). As a silver source, two different precursor namely silver nitrate and silver chloride were used. It is found that addition of silver aggregates in the amorphous $SiO_2$ network promotes partial crystallization of silica as cristobalite. For the samples in which silver nitrate is used as a source of silver aggregate, the cristobalite phase was observed at heat treatment temperatures as low as 600°C. On the other hand, for the samples with silver chloride, the cristobalite phase appeared at 800°C. In fact, no crystallization of $SiO_2$ was observed at temperatures below 1000°C for samples without silver. Garnica et al. observed similar result for samples without silver (Garnica et al. 2001). Another observation in their study was that broad diffraction line from amorphous $SiO_2$ became narrower together with a shift to a lower angle with heat treatment. This indicates the improvement in the structural short range ordering towards the cristobalite phase (Garnica-Romo et al. 2001). By comparing the crystallization behavior of the samples with and without silver, it can be said that the presence of metal disrupts the amorphous network which reduces the kinetic barrier to crystallization. Moreover, this effect is more pronounced in the samples loaded with silver nitrate (Ortega-Zarzosa et al. 2003).

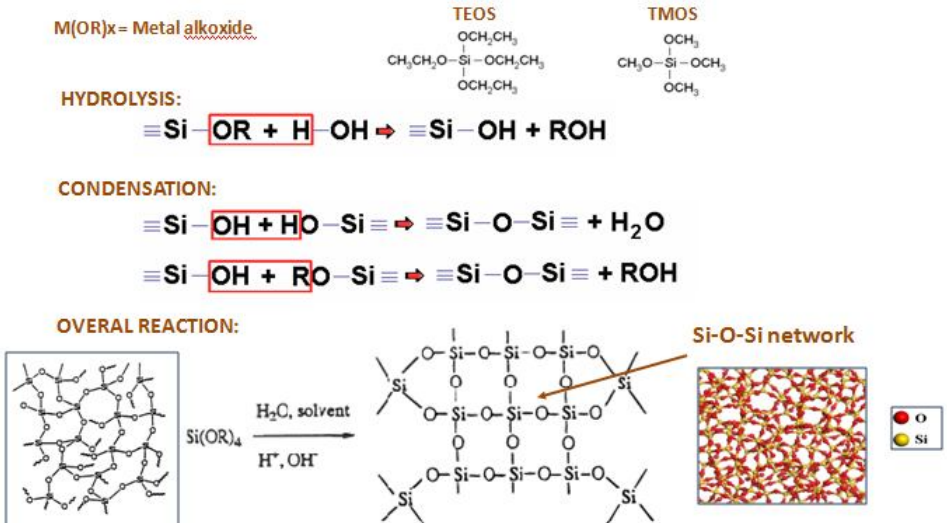


**Figure 1.2** Chemical reactions during gel formation in conventional sol-gel method (reproduced from Brinker and Scherer 1990).

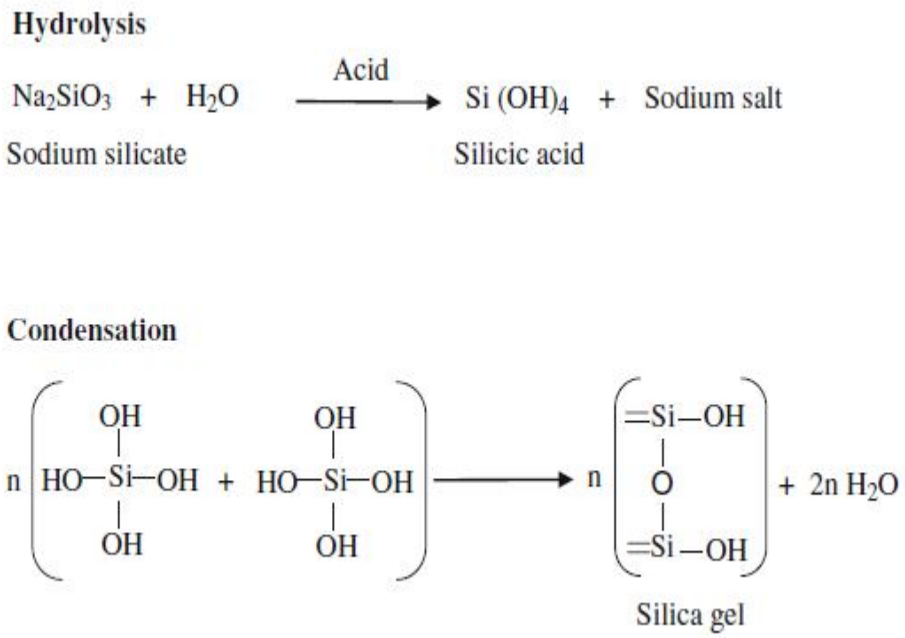


**Figure 1.3** Sol-gel transformation of sodium silicate to silica gel.

Ortega-Zarzosa et al. also found that the particle size of metallic silver colloids changes with annealing temperature (Ortega-Zarzosa et al. 2003). In order to achieve partial crystallization, metallic silver clusters should reach a size in the range of 75-80 nm. Ortega-Zarzosa et al. 2003 achieved silica gel to silica glass transformation above 500°C. In another study carried out by Garnica-Romo et al. 2002, similar result was obtained. In their study, the crystallization of $SiO_2$ coating into the cristobalite phase occured at temperatures as low as 500°C. According to their study, it is found that silver needs to be in a critical amount such that it forms metallic particles initiating crystallization into the cristobalite phase. As an another requirement, $SiO_2$ samples should be prepared from precursor solutions with high $H_2O$/TEOS ratios (Garnica-Romo et al. 2002).

In literature, there are reports about spontaneous reduction of silver ions (Mennig et al. 1992; Ritzer et al. 1997; Renteria et al. 1998). According to these reports, silver may precipitate even during the sol-gel transitions. Wu et al. 2000 studied the mechanisms responsible for spontaneous silver precipitation in sol-gel derived silver-doped silica materials. In their study, HCl solutions with different concentrations were mixed with aqueous $AgNO_3$ solution. Scattering-like behavior which was strongly dependent on the HCl concentration was observed in optical absorption. The scattering was because of suspended particles that is formed after mixing. Characterization results indicated that precipitates were silver chloride. The precipitation of silver chloride is due to low solubility of AgCl in the aqueous solution. In fact, the silver ion concentration in the final wet gel was reported to be well above the solubility limit. Therefore, it can be said that the concentration of the catalyst, HCl, is the factor causing precipitation of AgCl. It is also known that the AgCl microcrystals are photosensitive and produce silver nanoparticles upon exposure to the ambient light. As a result, scattering-like absorbance changes the silver plasma absorption band (Wu et al. 2000).

Renteria et al. 1998 investigated the influence of temperature on the color stability and also the effect of ethanol on the stability and aggregation properties of silver colloid containing gels. In samples without ethanol, an optical reversibility phenomenon was observed which can be attributable to silver atom colloids that are oxidized to $Ag_2O$ (De et al. 1996; Mennig et al. 1997; Ritzer et al. 1997). At temperatures above 400°C, this phenomenon can also be explained by aggregation-collapse of the colloidal silver particles. It can also be concluded that the use of ethanol in the preparation is an inhibiting agent in the formation of silver colloids (Renteria et al. 1998).

Silver containing silica glasses often show yellow or brown color due to existence of silver colloid particles. However, colorless and chemically durable materials with slow release of silver ion for a long period are more desirable for antibacterial applications. For this purpose, Kawashita et al. prepared antibacterial silver-containing glass by sol-gel method with the addition of $(Al(NO_3)_3).9H_2O$ to the solution of $Si(OC_2H_5)_4$, $AgNO_3$, $HNO_3$, $C_2H_5OH$ and $H_2O$ (Kawashita et al. 2000). In their study, at a constant Si/Ag atomic ratio, the effect of Al/Ag atomic ratio on color and chemical durability are investigated. With Al/Ag=0 atomic ratio, a yellow colored glass was obtained due to the existence of silver in the form of metallic colloids in the glass. On the other hand, for the compositions of Al/Ag≥1, colorless glasses were obtained. This is attributable to the existence of silver in the form of $Ag^+$ ions in these glasses. With the addition of $(Al(NO_3)_3).9H_2O$, aluminum ions are incorporated into the $SiO_4$ network structure in the form of $[AlO_4]^-$ tetrahedra. With

$Ag^+$ ions, the negative charge of $[AlO_4]^-$ should be compensated as a result of which $Ag^+$ ions are localized to the $[AlO_4]^-$ tetrahedra. This localization makes it difficult for silver to be in the form of colloid. Besides, it is also observed that in the glasses with Al/Ag=0 atomic ratio silver ions were easily released into the water whereas for the compositions of Al/Ag≥1, they were released into water at a controlled rate. In fact, this is related to release of silica ions. In the samples with Al/Ag=0, it is seen that silica ions were easily released from surfaces of powders as a result of which metallic silver colloids were exposed to water and then easily released. However, for the samples with Al/Ag≥1, silica ions were not easily released from powders. Only mechanism for the release of silver ions was ion exchange between $Ag^+$ ion and hydronium ($H_3O^+$) ion from surrounding water. Therefore release of $Ag^+$ ion is controlled by the rate of inter diffusion of these ions (Kawashita et al. 2000). In another study carried out by Kawashita et al., it is found that the concentration of the released silver ions increases with an increase in silver content (Kawashita et al. 2003).

Another parameter which effects the Ag-$SiO_2$ formation is $H_2O$/TEOS ratio. Garnica-Romo et al. suggested that the structure of the samples prepared from solutions with the low $H_2O$/TEOS ratio are more porous (Garnica-Romo et al. 2002). Therefore, the silver diffuses faster to form large aggregates. On the other hand, in the samples with the high $H_2O$/TEOS ratio, a more ordered and denser structure is observed which in turn limits the mobility of the silver atoms leading to a fewer and smaller particle formation. After silver nitrate thermally decomposed at temperatures of about 300°C, the diffusion and aggregation of silver occurs. It is also found that an increasing $H_2O$/TEOS ratio enhances the hydrolysis and condensation rates. As a result, samples with low water content form longer Si—O—Si chains together with a more open structure. However, those with larger water content form a more compact three-dimensional network (Garnica-Romo et al. 2002).

#### 1.1.5.2 Silver-doped silica coatings processed using organic precursor (TEOS)

Although there is no clear mechanism for formation of Ag-$SiO_2$ films, the transformation of terminal non-bridging Si—O groups into Si—O—Ag network by cation exchange (De et al. 1996; Bruni et al. 1999) according to:

$$\equiv Si-OH + Ag^+ \rightarrow \equiv Si-O-Ag + H^+$$

is one of the well accepted mechanisms. According to a study carried out by Jeon et al., elimination of residual organic compounds results in densification of silica network (Jeon et al. 2003). Moreover, devitrification of amorphous $SiO_2$ sol-gel samples with silver is promoted by thermal treatments. When films were calcined at low temperatures, below 600°C and exposed to natural light, they turn into dark color. This was attributed to the presence of silver ions after heat treatment which are not reduced to metallic silver during calcination at temperatures lower than 600°C. By an increase in calcination temperature, metallic silver nanoparticles efficiently form in $SiO_2$ network (Jeon et al. 2003).

Ag-$SiO_2$ films have different colors according to calcination; basically related to the chemical state of silver temperature. Explanation for this phenomenon is that the silver particles may be oxidized to $Ag_xO_y$ above 400°C (but below 600°C), and reduced to silver particles at 600°C. As-produced films have yellowish color at room temperature. As temperature rises to 200-300°C color becomes dark brown because $Ag^+$ ions form $Ag_xO_y$ compounds. Above 400°C, films become colorless. However, this bleaching effect is reversible. When they are exposed to light, they becomes yellow again. At above 600°C, color becomes stable because silver metal particles completely trapped in $SiO_2$ matrix (Mennig et al. 1997). However, some researchers support that darkening and bleaching is due to an aggregation-disaggregation of silver particles (Ritzer et al. 1997).

De et al. 1996 studied silver-doped silica films as a function of annealing atmosphere and temperature. According to their study, annealing in an air (oxidizing atmosphere) causes to a decrease in the melting temperature of silver to a temperature as low as 650°C. This temperature is much lower than melting temperature of bulk silver which is 961°C. On the other hand, annealing in an inert (Ar) or reducing ($5\%H_2 - 95\%N_2$) atmosphere results in dissolution of clusters at about 900-950°C which is much closer to the melting temperature of bulk silver. It is also observed that when the annealing temperature increases, larger clusters break up into smaller units. Moreover, increase in annealing temperature results in the migration of silver towards surface of the films in the case of coatings on glass (De et al. 1996).

#### 1.1.5.3 Silver-doped silica materials processed using inorganic precursor (sodium silicate)

In literature, there are few study on the silver-doped silica materials prepared from sodium silicate via alternative sol-gel method instead of conventional sol-gel method using TEOS (Serezhkina et al. 2003; Xing et al. 2007; Hilonga et al. 2009; Hilonga et al. 2010). Serezhkina et al. 2003 prepared Ag-$SiO_2$ films by sol-gel method in a two different ways. In the first way, the films were based on tetraethyl orthosilicate precursor while the others were based on sodium silicate precursor. The effect of the heat treatment temperature on the phase composition of Ag-$SiO_2$ films is investigated. Phase composition of the films based on tetraethyl orthosilicate differs from those based of sodium silicate although both films heat treated at 150°C contain $AgNO_3$ phase. Ag phase is observed after heat treatment at 350°C for the films based on tetraethyl orthosilicate whereas in the films based on sodium silicate, Ag phase occurs after heat treatment at 600°C. Another difference was observed in the crystallization of $SiO_2$. In tetraethyl orthosilicate based films, the cristobalite phase is observed after heat treatment at 500°C and quartz phase after 600°C. On the other hand, after heat treatment in the temperature range 350-500°C, sodium silicate based samples show amorphous structure. For the same samples, Ag and cristobalite phases appear after heat treatment at 600°C (Serezhkina et al. 2003). Xing et al. prepared an antimicrobial textile by using water glass precursor (Xing et al. 2007). In their study, first $SiO_2$ network prepared after which cotton textiles treated with silver nitrate solution. At the end, it is found that prepared textiles showed an excellent antimicrobial effect against *E. Coli*. The coated samples withstand 50 washing cycles without losing the antibacterial effect.Hilonga et al. investigated changes in silver states with increase in calcination temperature (Hilonga et al. 2009,2010). It is found that silver exists as a nanoparticle at 600°C whereas it exist in ionic form at higher temperatures. This was attributed to the same explanation with a study that Kawashita et al. carried out in the presence of aliminum source as mentioned earlier (Kawashita et al. 2000, 2003).

## 1.2 Objective of the thesis

The general objective of this study was to establish the processing routes for the development of antibacterial silver-doped silica powders from sodium silicate (water glass). Silver-doped silica powders has been obtained by sol-gel method.

The experimental work conducted in this thesis consists of two major tasks. In the first part, silica formation from sodium silicate (water glass) has been investigated. The gelation behavior and the time-dependent conversion from aqueous to solid (gel) form for sodium silicate:solution:water:catalyst formulations has been investigated. Accordingly, gel formation processes parameters for obtaining silica from sodium silicate solution were determined.

In the second part, silver-doped silica (Ag-$SiO_2$) powders were synthesized. This was achieved by two routes. The details of synthesis methods have been outlined and discussed. One of the selected routes was based on the findings of the initial gelation behavior studies in the first part. The effect of washing treatment on sodium removal from sol-gel derived silica gel powders has been discussed. In addition, the effect of the calcination temperature on the silver colloid formation behavior and the effect of silver crystallite size on the crystallization behavior of the silica matrix have been discussed.

# CHAPTER 2

# EXPERIMENTAL PROCEDURE AND MATERIAL CHARACTERIZATION

In this chapter, the chemicals/materials used and the experimental work conducted in the thesis are explained in detail.

## 2.1 Materials

All the chemicals used in the thesis for the synthesis of antibacterial Ag-$SiO_2$ powders and their sources are listed in Table 2.1.

**Table 2.1** The chemicals used in the experimental part of the study and their sources.

| **Material** | **Formula** | **Source** | **Molecular weight (g/mol)** | **Catolog Number** |
|---|---|---|---|---|
| Silver nitrate | $AgNO_3$ | Sigma-Aldrich | 169.87 | 7761-88-8 |
| Sodium silicate solution (water glass) | $Na_2SiO_3$ ($SiO_2$=26 wt.%, $Na_2O$=13 wt.%) | Kale Seramik, Turkey | 122.06 | n.a. |
| Nitric acid | $HNO_3$ | Merck | 63.01 | 100443 |
| Hydrochloric acid | HCl | Sigma-Aldrich | 36.45 | 7647-01-0 |

## 2.2 Experimental procedure

### 2.2.1 Silica formation from sodium silicate (water glass): gelation behavior and optimization of processing parameters

The processing flowchart for silica gelation/kinetics studies from sodium silicate solution is shown Figure 2.1. Wet gels were prepared from commercial (industrial grade, used in glaze applications) sodium silicate solution ($Na_2SiO_3$, water glass, Kale Seramik, Turkey, $SiO_2$=26 wt.%, $Na_2O$=13 wt. %) using hydrochloric acid (HCl, Merck) as acid catalyst. The sols were prepared by drop wise addition of HCl solution with three different molar concentrations (0.5, 1.0, 2.0 and 4.0 M, respectively) into aqueous sodium silicate solution under stirring. The pH value is measured continuously with a pH meter. Then, the sols were transferred into closed plastic containers for aging at room temperature up to 1 month to observe the gelation.

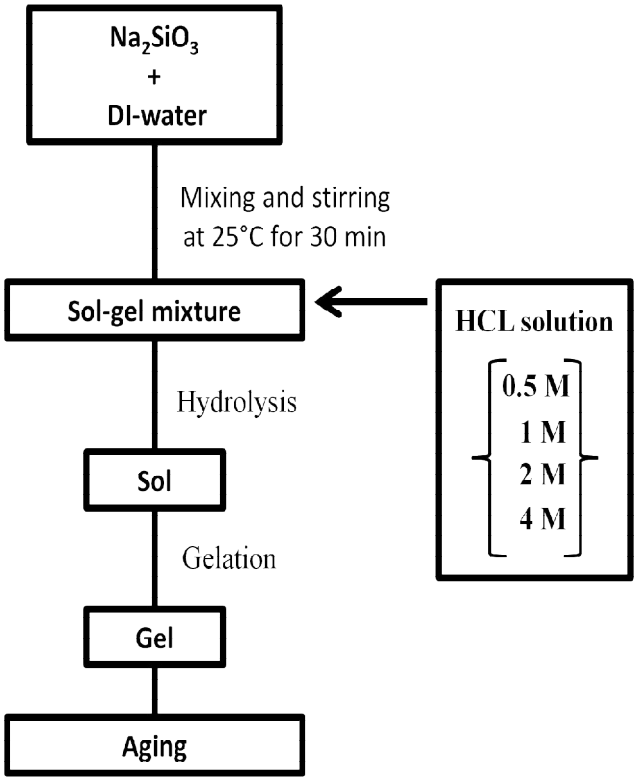


**Figure 2.1** Flowchart for the synthesis of silica from sodium silicate solution.

### 2.2.2 Preparation of sol-gel derived silver-doped silica (Ag-$SiO_2$) powders from sodium silicate (water glass) based systems

The silver incorporation into silica was attempted using two processing routes. In the first route, hereafter named as "indirect synthesis route", silver was incorporated into semi-mature gel form of silica aged in aqueous silver-ion containing solutions. In the second processing route called "direct synthesis route", silver was directly incorporated (by providing silver ions in the hydrolysis media, i.e. water) into the sol state prior to gelation. The details of the two processing routes are outlined in the following section.

#### 2.2.2.1 Indirect synthesis route

In this processing route, first, silica gel was prepared and then aged in silver nitrate solution. In the first step, 9 mL of sodium silicate solution ($Na_2SiO_3$, water glass) was mixed with 27 mL of DI-water. Then, 24 mL of 1 M nitric acid ($HNO_3$, Merck) solution was added drop wise into the solution. After complete addition, the sols were poured into polystyrene test tubes and sealed with Parafilm for gelation. Gelation occured in an approximately 2-3 min. After 1 week of aging, gels were washed with DI-water during 6 days in order to remove sodium from the system. The washing water was changed for every 24 hours. After the washing treatment, gels were exposed to silver nitrate solutions with two different concentration (0.01 and 0.02 M, respectively) for 2 weeks and then, they were dried at 70°C for 1 day. Then, dried gels were grinded. Finally, grinded powders were calcined at 200°C, 400°C, 600°C and 800°C in air for 2 h. Figure 2.2 illustrates the sol-gel processing flowchart of Ag-$SiO_2$ powders obtained by indirect synthesis route.

#### 2.2.2.2 Direct synthesis route

In this processing route, sol-gel mixtures were prepared by using silver containing aqueous solutions obtained by dissolving $AgNO_3$ in DI-water. This solution was then mixed with sodium silicate solution and catalyst. Two different formulations were prepared; with a moderate silver amount, $[AgNO_3]/[Na_2SiO_3]$=0.004 and higher concentration $[AgNO_3]/[Na_2SiO_3]$=0.008, respectively. The formulation and gelation times for this route are shown in Table 2.2. The experimental details for the preparation of the Ag-containing sol-gel systems are given in the next paragraph.

**Table 2.2** Formulation and approximate gelation times for silica gels obtained using direct synthesis route with **(a)** moderate concentration, $[AgNO_3]/[Na_2SiO_3]$ = 0.004 and **(b)** higher concentration, $[AgNO_3]/[Na_2SiO_3]$ = 0.008

| | **(a)** **Moderate concentration** **$[AgNO_3]/[Na_2SiO_3]$ = 0.004** | **(b)** **Higher concentration** **$[AgNO_3]/[Na2SiO_3]$ = 0.008** |
|---|---|---|
| ***Formulation*** | $[Na_2SiO_3]$:$[AgNO_3]$:$[H_2O]$:$[HNO_3]$ | $[Na_2SiO_3]$:$[AgNO_3]$:$[H_2O]$:$[HNO_3]$ |
| ***(Molar ratio)*** | 1 : 0.004 : 17 : 4 | 1 : 0.008 : 17 : 4 |
| ***Gelation time*** | 2-3 min | 2-3 min |

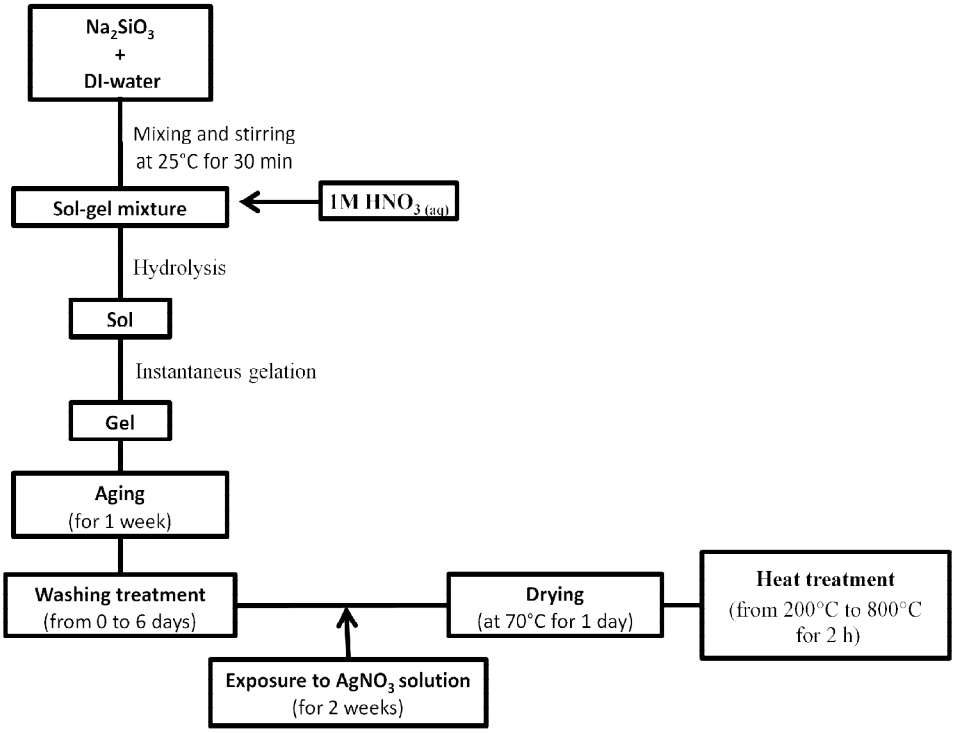


**Figure 2.2** Sol-gel processing flowchart of Ag-$SiO_2$ powders obtained by indirect synthesis route.

Sodium silicate solution ($Na_2SiO_3$, water glass) and silver nitrate ($AgNO_3$) were taken as the starting materials. DI-water was taken as a solvent and nitric acid ($HNO_3$, Merck) as an acid catalyst. In the first step, 0.07 g of $AgNO_3$ was dissolved in 4 ml of DI-water to form solution-A. In an another beaker, 9 mL of sodium silicate solution was mixed with 27 mL of DI-water to form solution-B. Then, solution-A was added into solution-B step by step under stirring. At the meantime, for every 1 mL of solution-A, 6 mL of 1 M $HNO_3$ solution was added drop wise into solution-B for each step. It is worth to mention that catalyst concentration was chosen based on the gelation/kinetics studies (section 2.2.1) to achieve the same solution conditions yielding gel products in relatively short time periods. After complete addition, the sols were poured into polystyrene test tubes and sealed with Parafilm for the gelation. The gelation occured in an approximately 2-3 min. After 1 week of aging, the gels were washed with DI-water during 6 days in order to remove sodium from the system. The washing water was changed for every 24 hours. After the washing treatment, the gels were dried at 70°C for 1 day. Then, the dried gels were grinded. Finally, the grinded powders were calcined at 200°C, 400°C, 600°C and 800°C in air for 2 h. Figure 2.3 displays the flowchart of the direct synthesis route.

## 2.3 Material characterization

### 2.3.1 Phase analysis/evaluation (x-ray diffraction analysis)

X-ray diffraction (XRD) analysis measurements were employed for the phase analysis of sol-gel derived silver-doped silica powders. The analysis were performed by Rigaku X-Ray diffractometer (Ultima D/MAX2200/PC). CuKα radiation was used as an X-ray source at 40 kV. The scan speed was 2°/min. the silver-doped silica powder samples were scanned over from 10º to 80º in 2θ.

### 2.3.2 Antibacterial activity (disc diffusion method)

The antibacterial activity of the Ag-$SiO_2$ powders was evaluated by the disk diffusion method aganist gram-positive bacteria *Staphylococcus Aureus* (ATCC 29213) and gram-negative bacteria *Escherichia coli* (ATCC 25922) were used as the indicator microorganism as summarized in Table 2.3. All materials were sterilized in an autoclave before the antibacterial test studies. Muller-Hinton agar (Merck) for testing the sensitivity of clinically important pathogens was used as a seeding environment of the bacteria culture during long-tem exposure of bacteria to the powder samples. For the agar preparation, first, 34 g agar was mixed with 1 L DI-water in order to obtain homogeneous solution and kept at 120°C under 3 atm pressure for 15 min in autoclave. When autoclave treatment finished, agar containing solution was cooled to 50°C. Then, agar:DI-water solution was poured into sterilized polystryene petri dishes. These agar containing petri dishes were hold at room temperature for 2-3 h and then, kept at 4°C in a refrigerator. After agar preparation step, long-term contact between the bacteria colonies and representative powder samples was achieved. For this purpose, bacteria colonies which had been frozen to -80°C was inocculated into agar containing petri dishes.by spreading with cultiplast and then, kept at 37°C for 1 day in order for colony dissociation.Finally, 0.025 g powder samples were spreaded down on the bacteria-seeded agar plate to generate a definite contact between agar and powder samples. The size of inhibition zones around the powder samples were measured after 3, 6 and 24 h, respectively. Figure 2.4 summarizes the antibacterial activity test in a schematic manner.

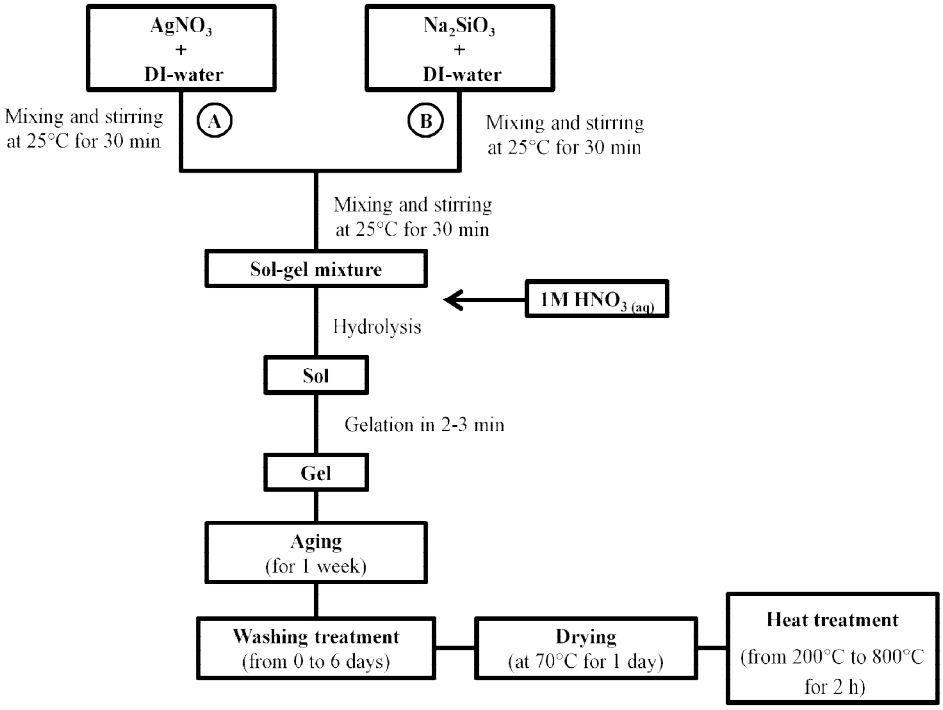


**Figure 2.3** Sol-gel processing flowchart of Ag-$SiO_2$ powders obtained by direct synthesis route.

**Table 2.3** Properties of the bacteria used in the antibacterial test of Ag-$SiO_2$ powders.

| **Organism** | **Strain** | **Characteristics** |
|---|---|---|
| *Staphylococcus aureus* | ATCC 29213 | Gram-positive |
| *Escherichia coli* | ATCC 25922 | Gram-negative |

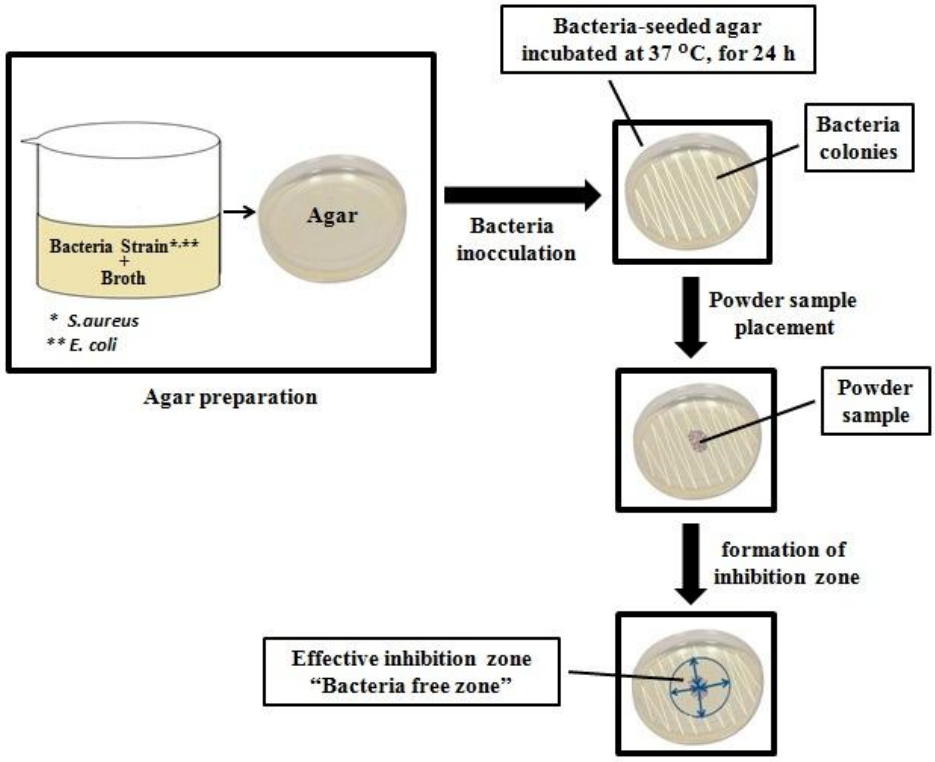


**Figure 2.4** Flowchart of the disc diffusion method for the evaluation of antibacterial activity.

# CHAPTER 3

# RESULTS AND DISCUSSION

## 3.1 Silica formation from sodium silicate (water glass): gelation behavior and optimization of processing parameters

In order to understand the silica formation from $Na_2SiO_3$-based aqueous solutions (plain silica gels without any silver incorporation), gelation behavior studies were performed as a preliminary experimental task. The gelation times were determined by visual inspection. Typically, four different distinct gelation behaviors were observed as shown by the representative images in Figure 3.1:

- (A-type) a clear/transparent solution without any gelation (Figure 3.1a)
- (B-type) a transparent gel with gelation leading to marginal syneresis (extra liqueurs $H_2O$ formation during gelation) during aging (Figure 3.1b)
- (C-type) an initial white gel with relatively faster gelation without any syneresis during aging (Figure 3.1c)
- (D-type) an initial white gel with extremely fast gelation without any syneresis during aging (Figure 3.1d)

In these studies, the formation of the "gel state" (B-, C- or D-type gel) or the gelation time ($t_g$) refers to the time span, at which the solution surface remain in contact with the container wall rather than free flowing/deforming and forming a meniscus like surface when the sample in the polystyrene container tilted 45°.

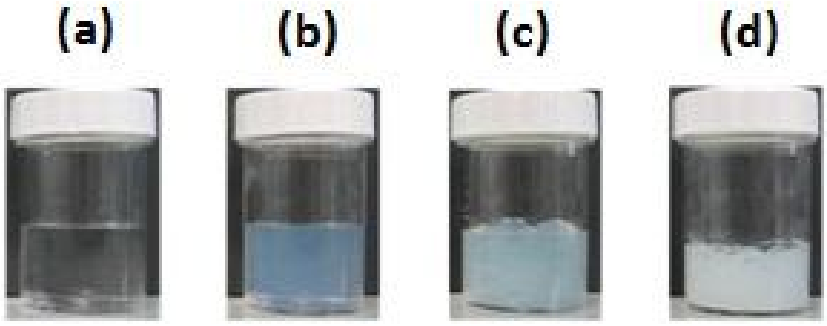


**Figure 3.1** Representative images for four different gelation behavior/type for plain silica gels obtained from $Na_2SiO_3$-based solutions. (a) a clear solution with no gelation (A-type), (b) a transparent gel with gelation leading to syneresis during aging (B-type), (c) an initial white gel with relatively faster gelation without any syneresis during aging (C-type) and (d) an initial white gel with extremely fast gelation without any syneresis during aging (D-type).

During the silica gel formation/gelation behavior studies, three different sets of samples were investigated. All of the samples were obtained from sodium silicate solution ($Na_2SiO_3$, water glass). In set A, the effect of the catalyst concentration (acid, $HCl_{(aq)}$) on the gelation behavior was studied using different molarities of HCl solutions; 0.5, 1.0, 2.0 or 4.0 M HCl. Then, in set B, silica gels were prepared using the optimum catalyst concentration as determined from the observations/findings on gelation of set A using various amount of sodium silicate precursor solutions corresponding different silica amount in the final formulation as 1 wt.% $SiO_2$, 2 wt.% $SiO_2$ and 4 wt.% $SiO_2$, respectively. This study was performed to investigate the effect of $SiO_2$ content percentage on the gelation behavior. Finally, in set C, the gelation behavior of $Na_2SiO_3$:$H_2O$:catalyst formulations has been also investigated by the pH measurements.

Figure 3.2 shows the gelation behavior of the silica gels in set A. Samples of set A were prepared from $Na_2SiO_3$:$H_2O$ mixtures with the same volume ratio of 1:1 (i.e. 3 mL:3mL of $Na_2SiO_3$:$H_2O$ ) by the addition of 20 mL catalyst with different concentrations (with 0.5, 1.0, 2.0 and 4.0 M HCl solution, respectively). As can be seen in Figure 3.2a, a clear solution with no gelation (A-type) was observed for the samples catalyzed with 0.5 M HCl solution. Gelation never occurred even after 1 month of aging period. On the other hand, an initial transparent gel with gelation (B-type) occurred in as-prepared condition for the samples catalyzed with 1.0 M HCl solution. For these samples, an initial transparent gel turned into a white gel after 1 h of aging period leading to some syneresis (formation liqueurous water upon hydrolysis reaction) after 1 day and more syneresis was observed after 1 month of aging period as illustrated in Figure 3.2b. Moreover, for the samples catalyzed with 2.0 M HCl solution, an initial white gel with fast gelation (C-type) was obtained in as-prepared condition and syneresis was never observed even after 1 month of aging period as shown in Figure 3.2c. Similarly, an initial white gel with very fast gelation (D-type) was observed in as-prepared condition for the samples catalyzed with 4.0 M HCl solution. Also, there was no syneresis even after 1 month of aging period as can be seen in Figure 3.2d.

In the light of these results, it is obvious that as the catalyst molarity increases, the gelation time gets shorter. However, gelation behavior also changes when the gelation time shortens. For instance, although gelation was observed for the samples catalyzed with 2.0 M and 4.0 M HCl solution, an instantaneous fast (very fast) gelation in these gels and no syneresis even after 1 month of aging period indicating an uncontrolled gelation behavior for these samples. On the other hand, a more controlled gelation behavior was observed for the samples catalyzed with 1.0 M HCl solution in comparison to the other samples as can be understood from Figure 3.2. In the case of poor catalysis conditions (0.5 M HCl catyalzed formulations) a rigid solid mass formation was never observed even after a month of aging.

Based on the observations for set A, it can be concluded that optimum gelation, i.e. formation of a wet semi-rigid form, was obtained for $Na_2SiO_3$:$H_2O$ mixture with volumetric mixing ration of 1:1 (i.e. 3 mL:3mL of $Na_2SiO_3$:$H_2O$) when catalyzed with 1.0 M HCl solution. Gelation takes place at around 1h for this specific formulation.

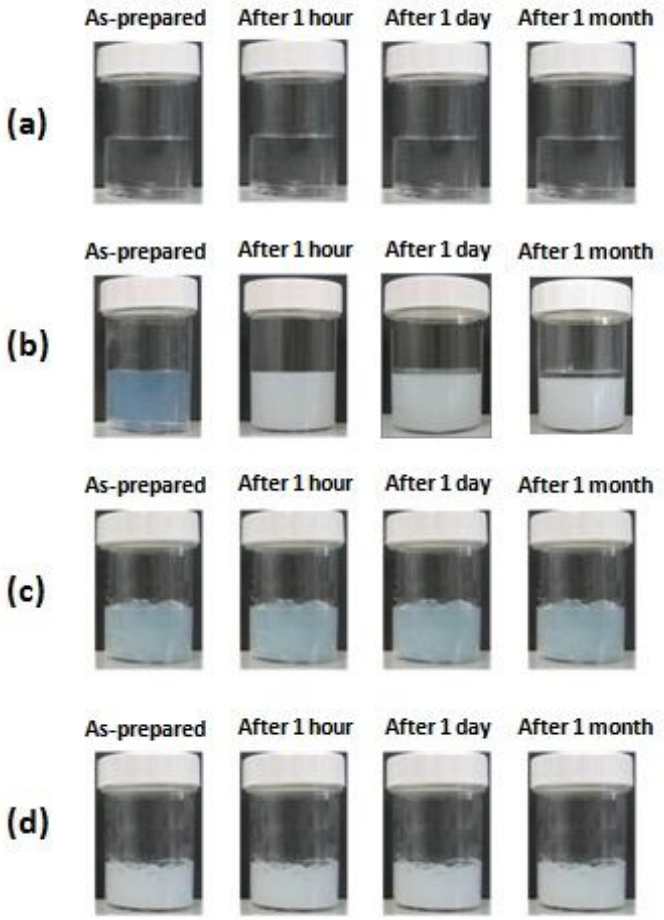


**Figure 3.2** The gelation behavior of the silica gels in set A prepared from $Na_2SiO_3$:$H_2O$ mixture with a volumetric mixing ratio of 1:1 (3 mL:3 mL of $Na_2SiO_3$:$H_2O$) catalyzed with **(a)** 0.5, **(b)** 1.0, **(c)** 2.0 and **(d)** 4.0 M HCl solution.

Figure 3.3 illustrates the gelation behavior of the silica formulations for set B. The formulations were determined to have a total $SiO_2$ content of 1 wt.% $SiO_2$, 2 wt.% $SiO_2$ and 4 wt.% $SiO_2$. In order to prepare solutions with the respective $SiO_2$ weight percentages, three different $Na_2SiO_3$:$H_2O$ mixtures with different dilution extent, i.e. 1:30, 1:10 and 1:1 (volume based) were prepared. This corresponds to 3 mL:90 mL, 3 mL:30 mL and 3 mL:3 mL of $Na_2SiO_3$:$H_2O$ mixtures. All mixtures were then catalyzed with 1.0 M HCl (20 mL) solution considering the optimum catalyst concentration determined in set A. For the samples with 1 wt.% $SiO_2$, gelation never occurred even after 1 month of aging (A-type) as shown in Figure 3.3a. However, gelation of the samples with 2 wt.% $SiO_2$ was observed before the first day of aging, exhibiting a B-type (gelation with syneresis) gelation as can be seen in Figure 3.3b. Similarly, it is shown in Figure 3.3c that a transparent gel (B-type gelation) developed in as-prepared condition without any aging for the samples with 4 wt.% $SiO_2$.

According to the experimental observations in set B, it is obvious that the higher $SiO_2$ content, the gelation of sodium silicate solution ($Na_2SiO_3$, water glass) occurs faster. Also, optimum gelation was observed for the samples with 4 wt.% $SiO_2$ i.e. $Na_2SiO_3$:$H_2O$ mixtures with the volume ratio of 1:1 which corresponds to 3 mL:3mL of $Na_2SiO_3$:$H_2O$ mixture. So, it can be said that an optimum silica precursor:$H_2O$ mixing ratio is required for controlling the behavior. An equal volumetric mixing ratio of these two components seems to be an effective choice for achieving gelation in practically relevant aging times (approx. 1 h). These results are somewhat consistent with the findings from set A.

In order to further understand the chemical factors controlling the gelation behavior sodium silicate, selected $Na_2SiO_3$:$H_2O$:catalyst formulations has been also investigated by the pH measurements. Accordingly, in set C, three different $Na_2SiO_3$:$H_2O$ mixtures of different dilution extent, i.e. 1:3, 1:10 and 1:20 (volume based) were prepared. This corresponds to 3 mL:9 mL, 3 mL:30 mL and 3 mL:60 mL of $Na_2SiO_3$:$H_2O$ mixtures. All mixtures were catalyzed either with 1.0 M or 2.0 M of HCl solutions and pH change as a function of added catalyst amount was monitored until gelation point. The initial and final pH values for the samples in set C are tabulated in Table 3.1.

**Table 3.1** The initial and final pH values for the samples in set C

| **$Na_2SiO_3$:$H_2O$ volume ratio** | 3 mL:9 mL | | 3 mL:30 mL | | 3 mL:60 mL | |
|---|---|---|---|---|---|---|
| **HCl molarity** | 1 M | 2 M | 1 M | 2 M | 1 M | 2 M |
| **Initial pH value** | 12.68 | 12.10 | 12.30 | 12.33 | 12.15 | 12.26 |
| **Final pH value** | 11.42 | 10.59 | 11.13 | 9.10 | 10.97 | 2.45 |

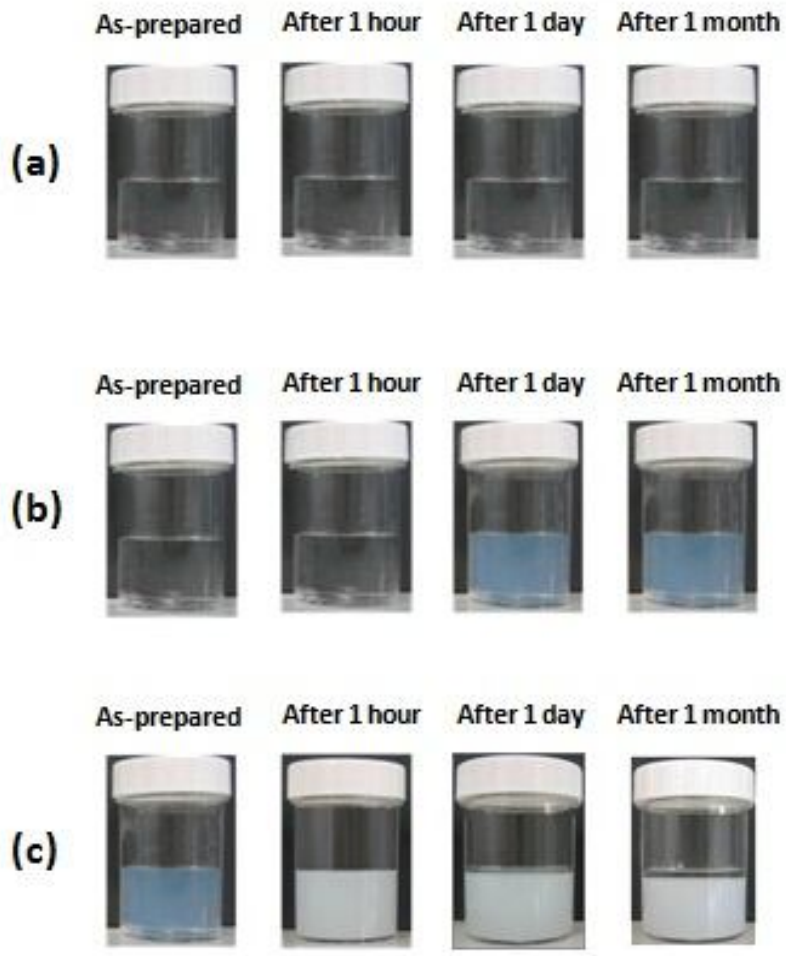


**Figure 3.3** The gelation behavior of the silica gels in set B prepared with three different $Na_2SiO_3$:$H_2O$ mixtures with different dilution extent; **(a)** 3 mL:90 mL (i.e. 1 wt.% $SiO_2$), **(b)** 3 mL:30 mL (i.e. 2 wt.% $SiO_2$) and **(c)** 3 mL:3 mL (i.e. 4 wt.% $SiO_2$) of $Na_2SiO_3$:$H_2O$ mixtures. All mixtures were catalyzed with 1 M HCl solution

Figure 3.4 shows the solution pH as a function of catalyst (1.0 M or 2.0 M HCl solution) amount added into the 3 mL:9 mL, $Na_2SiO_3$:$H_2O$ mixture, which is the most concentrated mixture in terms of silica precursor content, here sodium silicate solution ($Na_2SiO_3$, water glass). As can be seen from Figure 3.4, pH value decreases slightly from nearly 12.50 to 12.00 when 12 mL of 1.0 M HCl solution is added. On the other hand, lower pH value of 10.50 was obtained when only 4 mL of 2 M HCl solution was added into the mixture. For both samples (1.0 M or 2.0 M HCl solution), B-type gelation was observed at the end of HCl solution addition as represented by the inset image in Figure 3.4. Meanwhile, for relatively more diluted $Na_2SiO_3$:$H_2O$ mixture (i.e. 3 mL:30 mL of $Na_2SiO_3$:$H_2O$) a more steep pH drop was observed, as shown by Figure 3.5. In this case, an initial white gel with fast gelation (C-type) was observed for both samples (1.0 M or 2.0 M HCl solution) as shown by the inset of Figure 3.5. The final pH just before gelation was around pH=9.0. Furthermore, for the minimum diluted mixture with $Na_2SiO_3$:$H_2O$ ratio of 3 mL: 60 mL much more distinct and steeper pH drop was observed as shown by the data given in Figure 3.6. However, for the most diluted mixture with $Na_2SiO_3$:$H_2O$ ratio of 3 mL: 60 mL, gelation never occurred even at pH≈3 for both samples (1.0 M or 2.0 M HCl solution) as represented by inset of Figure 3.6.

The pH measurement based experimental results revealed that the catalyst is relatively more effective for the diluted mixtures of $Na_2SiO_3$:$H_2O$ sol-gel mixtures in achieving lower pH values. The different gelation behavior observed for sodium silicate solution of Set C can be explained by an analogy with the gelation kinetic model proposed for the silica gels formed by hydrolysis and condensation of silicon alkoxide (TEOS, tetraethyl orthosilicate) illustrated in Figure 3.7. This graph basically shows the relative rates of the chemical reactions as a function of solution pH. These reactions are *hydrolysis* (formation of hydrated silica species, silanols, Si–OH) and subsequent *condensation* (polymerization of the Si–OH species) reactions eventually and collaboratively leading to formation of solid silica (formation of Si–O–Si network) form at the end. The relative rates of both reactions are strongly regulated by the pH. The pH-dependent changes in these reactions can be related to the findings of current study to explain differences in gelation behavior of sodium silicate solutions. The pH value at the gelation point seems to be the primary factor for gelation and in defining the overall gelation time. For example, for the formulations with 3 mL:9 mL, $Na_2SiO_3$:$H_2O$ mixture, which is the most concentrated mixture in terms of sodium silicate solution ($Na_2SiO_3$, water glass), exhibiting a gelation (B-type) the final gelation occurred at highly alkaline conditions, 10.50-11.50, where both hydrolysis and condensation rate are relatively high as depicted by Figure. 3.7. Similarly, gelation (C-type) was observed for relatively more diluted $Na_2SiO_3$:$H_2O$ mixture (i.e. 3 mL:30 mL of $Na_2SiO_3$:$H_2O$) at the pH range of 9-9.50, where both hydrolysis and condensation reactions are still high. However, it is not clear why this specific formulation galled faster, even the combined rates are relatively slower compared to the former concentrated formulation. On the other hand, for the minimum diluted mixture with $Na_2SiO_3$:$H_2O$ ratio of 3 mL: 60 mL, gelation never occurred for a final pH≈3 due to the fact that the hydrolysis reaction rate is quite low, and do not proceed at all, simply delaying the gelation.

At the end of preliminary gelation behavior studies, based on the experimental observation of set A, set B and set C, a specific sol formulation for the sodium silicate precursor was determined. This corresponds to a $Na_2SiO_3$:$H_2O$:catalyst formulation of 3 mL:3 mL:20 mL. An optimum gelation, gelation at around 1 h, occurs when moderately strong catalyst (1.0 M HCl) solution producing a final gelation pH of 10.50-11.50 is used.

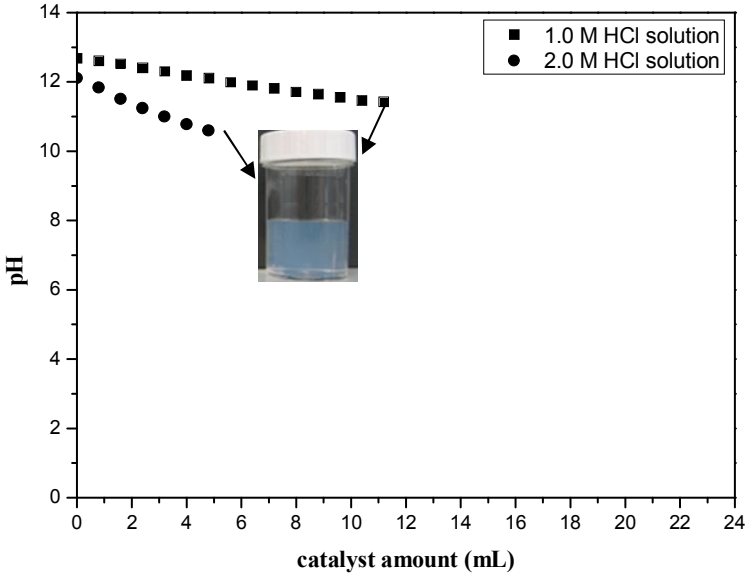


**Figure 3.4** The graph showing catalyst amount (HCl solution, 1.0 M or 2.0 M) for the sol-gel mixtures with $Na_2SiO_3$:$H_2O$ ratio of 3 mL:9 mL versus pH.

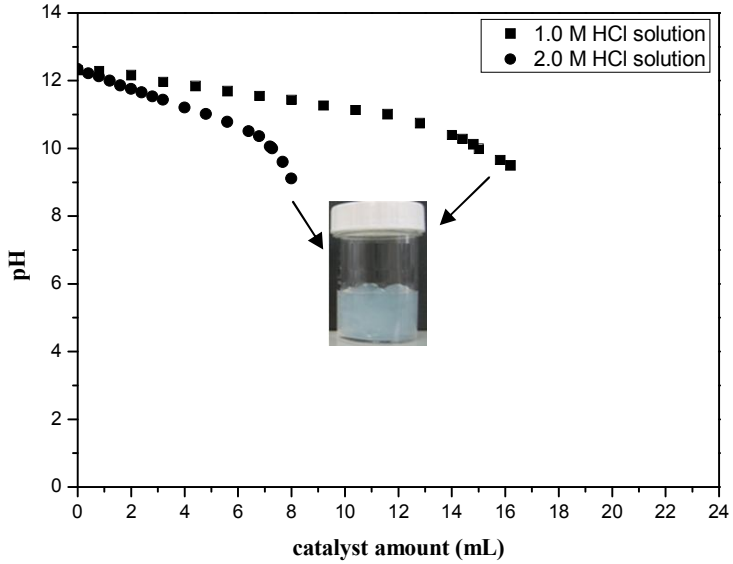


**Figure 3.5** The graph showing catalyst amount (HCl solution, 1.0 M or 2.0 M) for the sol-gel mixtures with $Na_2SiO_3$:$H_2O$ ratio of 3 mL:30 mL versus pH.

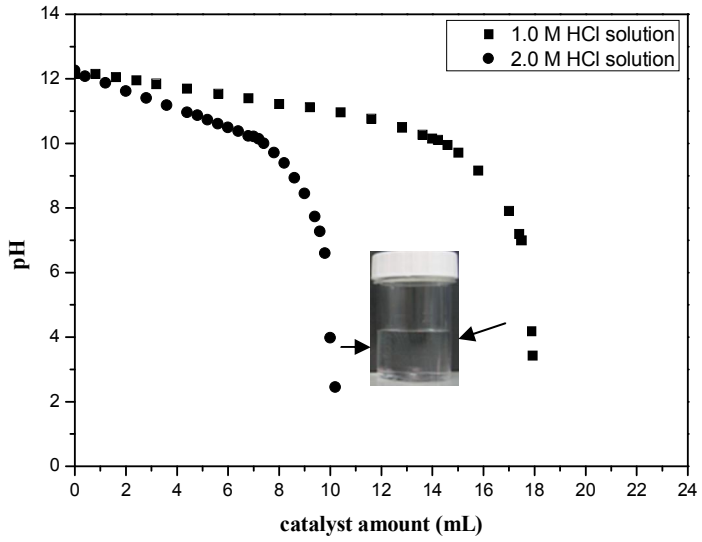


**Figure 3.6** The graph showing catalyst amount (HCl solution, 1.0 M or 2.0 M) for the sol-gel mixtures with $Na_2SiO_3$:$H_2O$ ratio of 3 mL:60 mL versus pH.

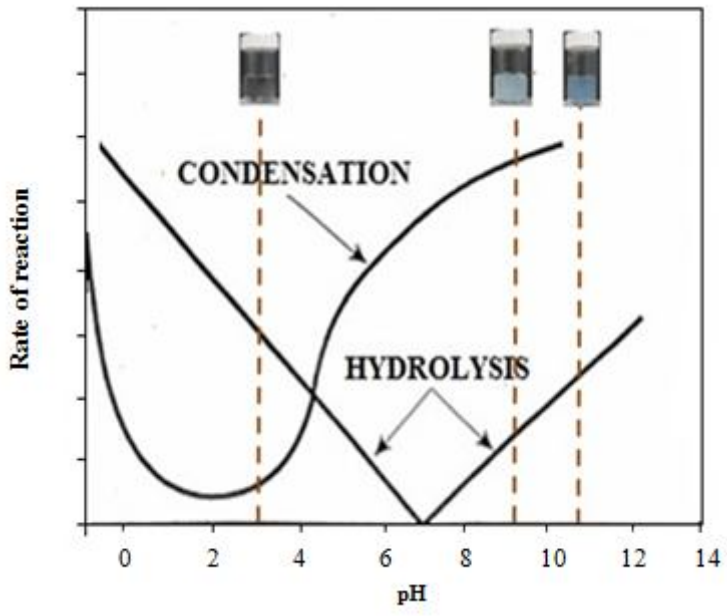


**Figure 3.7** The graph showing pH versus rate of hydrolysis and condensation reactions rates (reproduced from Brinker and Scherer 1990).

In the light of the silica gel formation/gelation behavior studies, sol-gel derived antibacterial silver-doped silica powders were synthesized in the following experimental studies. However, nitric acid ($HNO_3$) catalyst solution was used instead of HCl in the following studies for obtaining plain silica gels, which have been exposed to silver containing solutions for this purpose. This replacement was done intentionally due to possible precipitation chance of silver ions in the form of AgCl in silver containing sol-gel components. In these new formulations, the solution chemistry and the proportions of the solution components have been adapted from the HCl-based model studies of this section.

## 3.2 Characterization of sol-gel derived silver-doped silica (Ag-$SiO_2$) powders from sodium silicate (water glass) based systems

This section consists of two experimental results parts. In the first part, the effect of washing treatment on sodium removal from sol-gel derived silica gel powders has been reported. This study was performed for silica gels prepared using indirect synthesis route. A standard calcination procedure was performed on the gelled products (at 600°C in air for 2 h). Phase analyses (XRD) of the powders were done to understand the chemical changes during the washing treatment to eliminate Na-based components from gels obtained from sodium silicate precursors.

In the second part, sol-gel derived silver-doped silica (Ag-$SiO_2$) powders were prepared by two different processing routes namely indirect synthesis and direct synthesis route and the powders were heat treated at 200°C, 400°C, 600°C and 800°C in air for 2 h. Phase analyses (XRD) of the powders were done in order to investigate the changes during the high temperature calcination treatments. The phase identification of the powders both in "as-prepared" condition and "after calcination" treatments is presented. In addition, the effect of the calcination temperature on the silver colloid formation behavior and the effect of silver crystallite size on the crystallization behavior of the silica matrix are also discussed in the second part of this section.

### 2.3.1 Effect of washing treatment on the structural properties of Ag-$SiO_2$ powders

Washing treatments were employed to determine the extent of sodium removal from the sodium silicate based undoped and silver-doped powders. Figure 3.8 shows the XRD diffractograms of the sol-gel derived undoped silica powders ($[AgNO_3]/[Na_2SiO_3]=0$) after calcination in air at 600°C for 2 h. Figure 3.8a presents the XRD patterns of as-prepared samples (reference sample) which was not washed at all, and Figure 3.8b, 3.8c and 3.8d exhibits the XRD data of the samples after 2, 4 and 6 days of washing treatment, respectively. For the reference sample, eleven peaks assigned to $NaNO_3$ (nitratine) (JCPDS card no. 72-0025) at $2\theta$ = 22.82°, 29.38°, 31.89°, 35.37°, 38.95°, 42.52°, 47.92°, 48.36°, 56.46°, 58.72° and 63.50° are present as illustrated in Figure 3.8a. After 2 days of washing treatment, only the two strongest peaks assigned to $NaNO_3$ (nitratine) at $2\theta$ = 22.82° and 29.38° are observed. The other low intensity diffraction peaks of $NaNO_3$ were disappeared. The disappearance of $NaNO_3$ (nitratine) phase suggests that sodium is completely removed from the sol-gel derived undoped silica powders after 4 days of washing treatment. For the samples after 4 days and 6 days of washing treatment, only a broad peak ($2\theta \approx$ 15-25°) representing an amorphous silica network was detected.

Figure 3.9 exhibits the XRD diffractograms of Ag-$SiO_2$ powders obtained by indirect synthesis route and calcined in air at 600°C for 2 h containing low silver dopant concentration of $[AgNO_3]/[Na_2SiO_3]$=0.004. For the reference sample (unwashed), eleven peaks are present at 2θ = 22.82°, 29.38°, 31.89°, 35.37°, 38.95°, 42.52°, 47.92°, 48.36°, 56.46°, 58.72° and 63.50° corresponding to $NaNO_3$ (nitratine) (JCPDS card no. 72-0025) together with a peak at around 38° assigned to metallic silver (JCPDS card no. 4-0783). After 2 days of washing treatment, only three peaks assigned to $NaNO_3$ (nitratine) at 2θ = 29.38°, 35.37° and 42.52° remain with the decrease in the peak intensity and it is observed that the other eight peaks initially present and assigned to $NaNO_3$ (nitratine) disappear. As can be understood from Figure 3.9c, sodium is completely removed after 4 days of washing treatment. Furthermore, although metallic silver peak at around 38° remain after 2 days of washing treatment, it disappears after 4 days of washing treatment. Disappearance of both $NaNO_3$ (nitratine) and metallic silver peak after 4 days and 6 days of washing treatment indicates the removal of silver with sodium for the Ag-$SiO_2$ powders obtained using direct synthesis route with low silver dopant concentration of $[AgNO_3]/[Na_2SiO_3]$=0.004 is also removed. This also indicates that thermal reduction of silver ions ($Ag^+ \rightarrow Ag^0$) in the starting sol-gel mixture easily was proceed leading to the formation of metallic silver particles within the silica network.

Figure 3.10 illustrates the XRD data of indirectly synthesized Ag-$SiO_2$ powders with high silver dopant concentration of $[AgNO_3]/[Na_2SiO_3]$=0.008. XRD diffractograms are similar to those shown in previous figure (Figure 3.9a); unwashed sample again pattern revealed eleven peaks assigned to $NaNO_3$ (nitratine) (JCPDS card no. 72-0025) at 2θ = 22.82°, 29.38°, 31.89°, 35.37°, 38.95°, 42.52°, 47.92°, 48.36°, 56.46°, 58.72° and 63.50°. Moreover, there is a peak at around 38° corresponding to metallic silver (JCPDS card no. 4-0783). Compared to Figure 3.9b of Ag-$SiO_2$ powders with low silver dopant concentration of $[AgNO_3]/[Na_2SiO_3]$=0.004, there are extra peaks at 2θ = 22.82°, 38.95°, 48.36° and 56.46° in addition to three peaks assigned to $NaNO_3$ (nitratine) at 2θ = 29.38°, 35.37° and 42.52°. In contrast to XRD data shown in Figure 3.9c, metallic silver peak at around 38° can be still observed even after 6 days of washing treatment. This indicates that metallic silver remained for the Ag-$SiO_2$ powders (calcined in air at 600°C for 2 h) obtained by indirect synthesis route when high amount of silver nitrate was employed in the starting formulation.

However, it is worth to mention that metallic silver may be present in both low and high amount silver containing samples calcined at temperature (600°C and 800°C) due to the intrinsic limitation of XRD for phase detection when limited amount of certain phase is present.

### 3.2.2 Effect of calcination temperature on the structural properties of Ag-$SiO_2$ powders

In order study the effect of the heat treatment on the structural properties, Ag-$SiO_2$ powders obtained using both indirect and direct synthesis routes were calcined in air for 2 h at 200°C, 400°C, 600°C and 800°C, respectively.

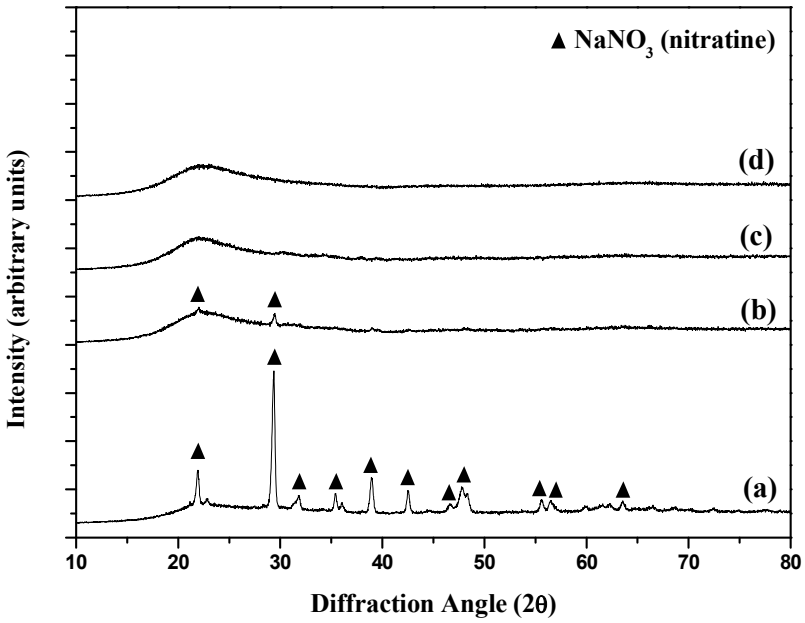


**Figure 3.8** XRD diffractograms of sol-gel derived undoped silica powders ($[AgNO_3]/[Na_2SiO_3]=0$) **(a)** in as-prepared condition (unwashed); after **(b)** 2 days, **(c)** 4 days and **(d)** 6 days of washing treatment. The calcination was performed at the same conditions in air at 600°C for 2 h.

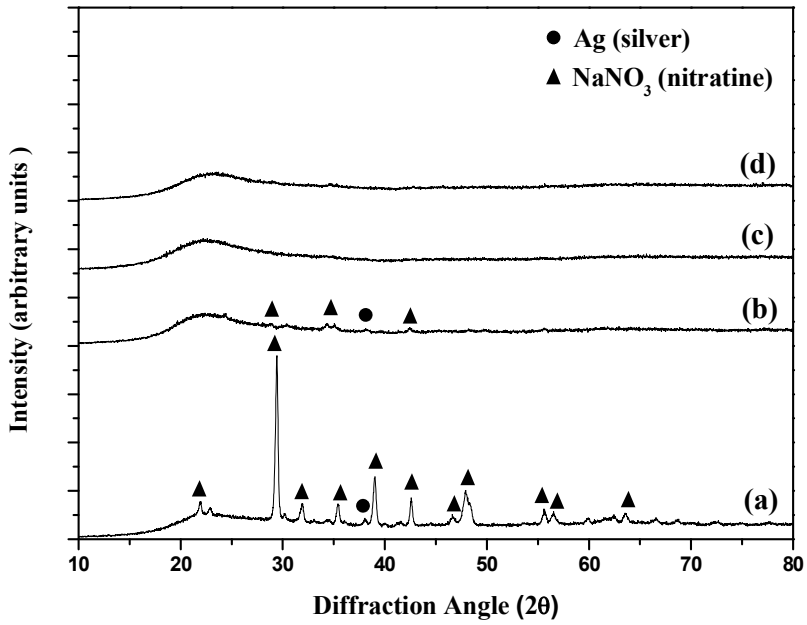


**Figure 3.9** XRD diffractograms of sol-gel derived silver-doped silica powders obtained using indirect synthesis route with low silver dopant concentration of $[AgNO_3]/[Na_2SiO_3]=0.004$ **(a)** in as-prepared condition (unwashed); after **(b)** 2 days, **(c)** 4 days and **(d)** 6 days of washing treatment. The calcination was performed at the same conditions in air at 600°C for 2 h.

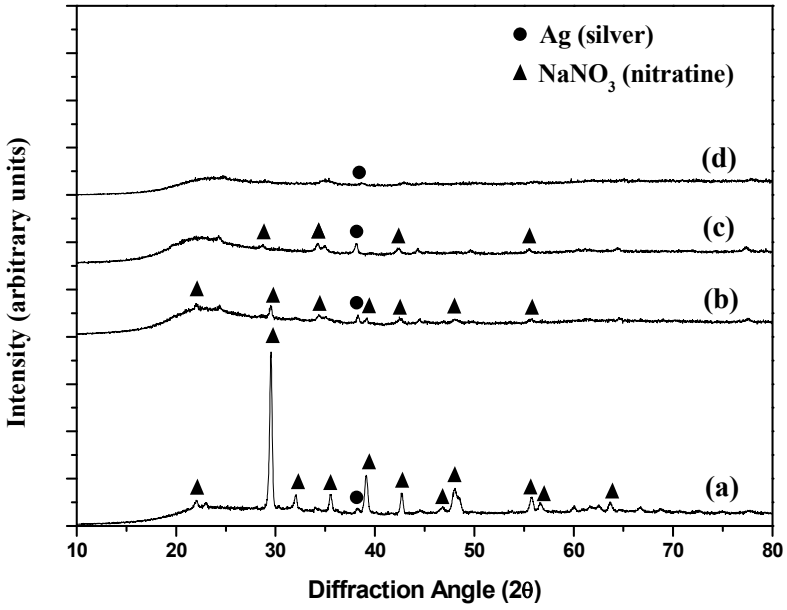


**Figure 3.10** XRD diffractograms of sol-gel derived silver-doped silica powders obtained using indirect synthesis route with high silver dopant concentration of $[AgNO_3]/[Na_2SiO_3]=0.008$ **(a)** in as-prepared condition (unwashed); after **(b)** 2 days, **(c)** 4 days and **(d)** 6 days of washing treatment. The calcination was performed at the same conditions in air at 600°C for 2 h.

Figure 3.11 discloses XRD diffractograms of sol-gel derived silver-doped silica powders obtained using indirect synthesis route. These samples were obtained by aging of wet gels were in a silver solution, of relatively low silver dopant concentration of 0.01 M $AgNO_3$. The XRD data are for the samples in as-prepared condition; after calcination at 200°C, 400°C, 600°C and 800°C for 2 h, respectively. For the samples obtained using indirect synthesis route exposed to low silver dopant concentration of 0.01 M $AgNO_3$ solution, only an amorphous silica network is observable up to 600°C as shown in Figure 3.11a, 3.11b and 3.11c, respectively. Four peaks at $2\theta \approx 38°$, 44°, 64° and 77° assigned to metallic silver (JCPDS card no. 4-0783) are present as depicted in Figure 3.11d. After calcination at 800°C, there exist a very weak intense peak at $2\theta \approx 22°$ representing cristobalite (JCPDS card no. 39-1425) indicating that amorphous silica network crystallizes into the cristobalite phase. Also, heat treatment at 800°C resulted in a distinct increase in the intensity of silver peaks as can be seen in Figure 3.11e. This increase can be explained by an increase in the extent silver formation by thermal reduction accompanied by of by an increasing silver particle at higher calcination temperatures.

XRD diffractograms of silver-doped silica powders obtained using indirect synthesis route exposed to high silver dopant concentration of 0.02 M $AgNO_3$ solution are illustrated in Figure 3.12. The samples in as-prepared condition (Figure 3.12a); after calcination for 2 h at 200°C (Figure 3.12b), 400°C (Figure 3.12c), 600°C (Figure 3.12d) and 800°C (Figure 3.12e) are shown. Only a broad peak ($2\theta \approx 15\text{-}25°$) representing the amorphous silica matrix is present until heat treatment of 600° as revealed in Figure 3.12 similar to the XRD data observed for the samples exposed to low silver dopant concentration of 0.01 M $AgNO_3$ solution. All of the silver diffraction lines at $2\theta \approx 38°$, 44°, 64° and 77° was observed for the samples of both heat treated at 600°C and 800°C with an increased intensity in the latter. In addition to silver peaks, the crystallization of amorphous silica to cristobalite was noticed as shown in Figure 3.12e. An important distinction between indirectly synthesized powders with different concentration is the difference in the high temperature crystallization trend of the amorphous silica network. This issue will be further clarified in the coming parts.

Figure 3.13 shows typical XRD diffractograms for Ag-$SiO_2$ powders prepared using direct synthesis route with low silver dopant concentration of $[AgNO_3]/[Na_2SiO_3]=0.004$. Patterns from samples in as-prepared condition; after calcination at 200°C, 400°C, 600°C and 800°C are illustrated. XRD diffractogram shown in Figure 3.13 reveals only a broad diffraction band centered at about 22° in the 2θ axis, which corresponds to the amorphous silica matrix, until heat treatment at 800°C. No other peaks including any silver peak are present as depicted in Figure 3.13a, 3.13b, 3.13c and 3.13d, respectively. As can be seen in Figure 3.13e, there exist a very weak intense peak at $2\theta \approx 22°$ representing the cristobalite phase (JCPDS card no. 39-1425) indicating that amorphous silica network crystallizes into the cristobalite phase after calcination at 800°C. This is an interesting observation. The crystallization of amorphous silica under normal conditions requires higher temperatures T>1000°C. There are also previous reports suggesting that the presence of silver particles promote crystallization of amorphous sol-gel derived silica matrix. [Ortega-Zarzosa et al. 2003, Akköprü and Durucan 2007]. Although no XRD peak indicating presence of silver after heat treatment of 800°C was observed, it is believed that silver metallic particles are present causing crystallization of amorphous silica network to cristobalite at 800°C.

Figure 3.14 shows the XRD data of the direct-synthesized Ag-$SiO_2$ powders with high silver dopant concentration of $[AgNO_3]/[Na_2SiO_3]=0.008$ for in as-prepared condition; after calcinations at 200°C, 400°C, .14c and 3.14d, respectively. There are also sign for presence of silver for the samples calcined 600°C and 800°C for 2 h, respectively. Similar XRD patterns with that of low silver dopant concentration were observed for the samples heat treated until 800°C as depicted in Figure 3.14a, 3.14b, 3at lower temperatures, however metallic silver diffractions are extremely low intensity. On the other hand, in the case of high silver dopant concentration, four peaks at $2\theta \approx 38°$, 44°, 64° and 77° assigned to metallic silver can be clearly seen for the sample calcined at 800 °C. The presence of metallic silver particles can be attributed to the high silver amount in these powders.

According to XRD-based phase analyses investigations of the Ag-$SiO_2$ powders in this section, it can be concluded that the extent of silver formation is higher for the indirectly synthesized powders. Formation of metallic silver particles at 600°C and higher silver peak intensity at 800°C for the indirectly synthesized powders support this conclusion.

Another important difference is the silica crystallization behaviors of the samples with low silver dopant concentration and high silver dopant concentration. Somewhat contrary to a study conducted by Akkopru and Durucan (2007), the crystallization of amorphous silica network was promoted for the samples with low silver dopant concentration instead of high silver dopant concentration. This difference can be explained with the size of silver particles. The synergetic effect of silver metallic particles on crystallization seems to be related with particle size rather than the quantity. The colloidal silver particles with smaller size are much effective and promote crystallization of the silica network. However, as the silver particles get bigger with increasing calcination temperature, either due to more efficient thermal reduction or other physical events leading to growth of the silver particles, this effect is suppressed. A possible scenario for the silver particle sizes achieved after calcination is shown in Figure 3.15. This figure schematically shows the silver particles size change as function of silver-amount for $SiO_2$-Ag samples heat treated at highest calcination temperature (800°C) employed in the current study. Both direct and indirect synthesis route samples with low and high silver amount are presented. The samples with low silver dopant concentration has always smaller silver particles compared to samples obtained with higher silver incorporation in the silica gel, which in turn improves crystallization of silica matrix. The reason for crystallization of silica in the presence of silver nanoparticles is clear. Some related this event to a heat localization effect as previously reported by Garnica-Romo et al. (2007).

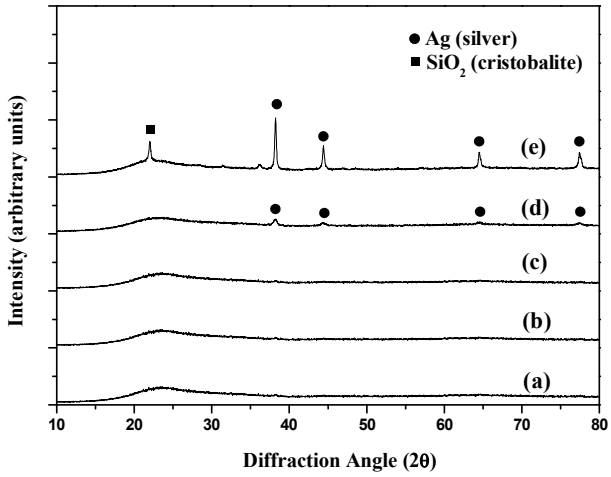


**Figure 3.11** XRD diffractograms of sol-gel derived silver-doped silica powders obtained using indirect synthesis route exposed to low silver dopant concentration of 0.01 M $AgNO_3$ solution **(a)** in as-prepared condition; after calcination at **(b)** 200°C, **(c)** 400°C, **(d)** 600°C and **(e)** 800°C for 2 h. The washing treatment was performed at the same conditions for 6 days.

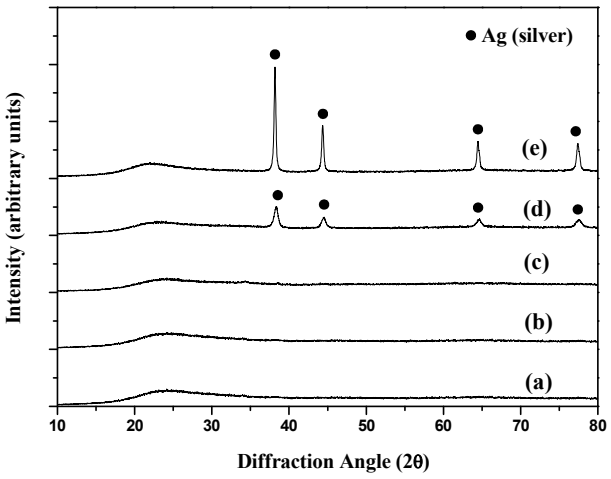


**Figure 3.12** XRD difractograms of sol-gel derived antibacterial silver-doped silica powders obtained using indirect synthesis route exposed to high silver dopant concentration of 0.02 M $AgNO_3$ solution **(a)** in as-prepared condition; after calcination at **(b)** 200°C, **(c)** 400°C, **(d)** 600°C and **(e)** 800°C for 2 h. The washing treatment was performed at the same conditions for 6 days.

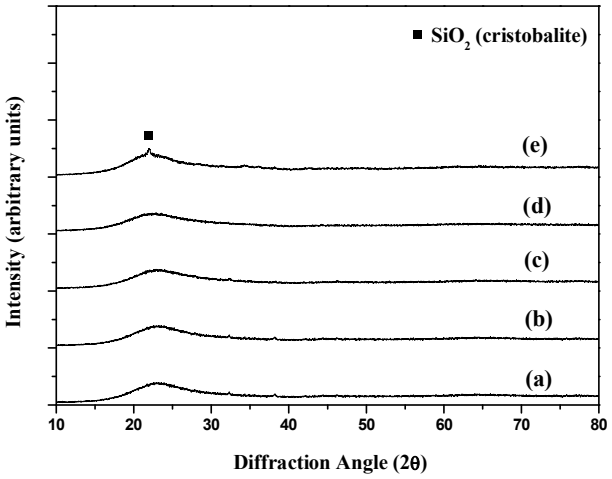


**Figure 3.13** XRD difractograms of sol-gel derived silver-doped silica powders obtained using direct synthesis route with low silver dopant concentration of $[AgNO_3]/[Na_2SiO_3]$=0.004 **(a)** in as-prepared condition; after calcination at **(b)** 200°C, **(c)** 400°C, **(d)** 600°C and **(e)** 800°C for 2 h. The washing treatment was performed at the same conditions for 6 days.

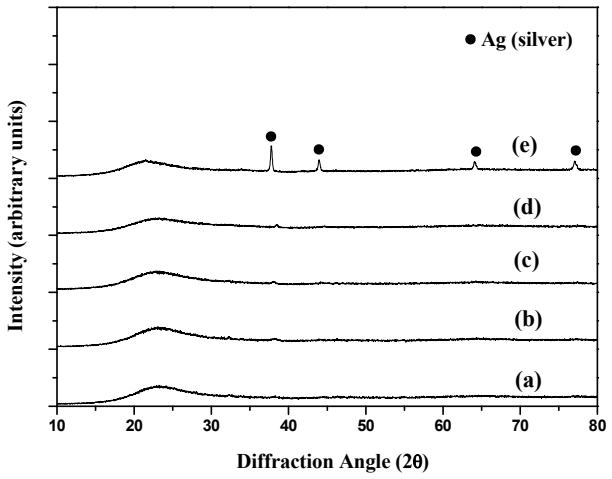


**Figure 3.14** XRD diffractograms of sol-gel derived silver-doped silica powders obtained using direct synthesis route with high silver dopant concentration of $[AgNO_3]/[Na_2SiO_3]$=0.008 **(a)** in as-prepared condition; after calcination at **(b)** 200°C, **(c)** 400°C, **(d)** 600°C and **(e)** 800°C for 2 h. The washing treatment was performed at the same conditions for 6 days.

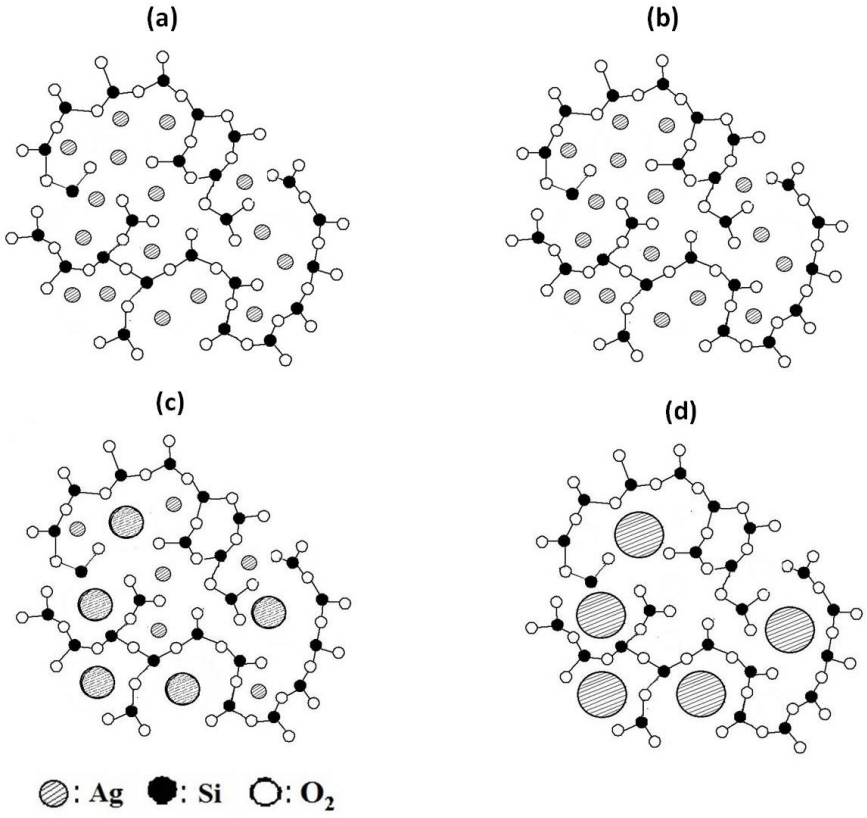


**Figure 3.15** Schematic illustrations of the possible mechanism on the formation of silver metallic particles after calcination at 800°C for **(a)** indirectly synthesized powders exposed to low silver dopant concentration of 0.01 M $AgNO_3$ solution, **(b)** directly synthesized powders with low silver dopant concentration of $[AgNO_3]/[Na_2SiO_3]=0.004$, **(c)** indirectly synthesized powders exposed to high silver dopant concentration of 0.02 M $AgNO_3$ solution and **(d)** directly synthesized powders with high silver dopant concentration of $[AgNO_3]/[Na_2SiO_3]=0.008$.

### 3.2.3 Antibacterial activity of Ag-$SiO_2$ powders

Antibacterial performance of the Ag-$SiO_2$ powders as a function of the bacteria strain type, silver dopant concentration and processing route were assessed by the disk diffusion method against *S. aureus* and *E. coli*. The images in Figure 3.16-3.19 reveal the antibacterial performance of of Ag-$SiO_2$ powders heat treated at 800°C on two different very common and generic bacteria. These images show the interaction between the powder surface and the bacteria containing agar (blue-colored background. The white linear features in these images are the bacterial colonies in/on the agar. The antibacterial performance of the powders was evaluated from the changes in the regions bordering between the powders samples and bacteria-seeded agar. This region will be referred as "inhibition zone", hereafter. The inhibition zone is the areal size of the dark and clear regions around the sample free of linear formations, i.e. bacterial colonies. In all antibacterial performance evaluations, the time-dependent antibacterial activity was investigated in by visual observations at 0 time; after 3, 6 and 24 h incubation against *S. aureus* and *E. coli*. It can be seen that all the samples at 0 time did not show antibacterial activity. After 3 h incubation, a clear the performance difference was observed for the two types of bacteria strains. The Ag-$SiO_2$ powders exhibit bactericidal activity against *E. coli* after 3 h incubation and the bactericidal effect almost remains the same even after 24 h incubation by revealing an approximately 1 mm of inhibition zone. On the other hand, the Ag-$SiO_2$ powders showed poor bactericidal effect against *S. aureus*, and after 3 h incubation and inhibition zone becomes more clear and bigger, reaching an approximate inhibition zone of 2-3 mm after 24 h (except for the samples shown in Figure 3.18a because of the powder scattering during the test preparation).

The important distinction between the antibacterial performances of Ag-$SiO_2$ powders against two different bacteria strains can be attributed to the difference in physical properties, i.e. cell wall structure and thickness. In general, *E. coli* (gram-negative bacteria) is more susceptible to silver particles than S. aureus (gram-positive bacteria) due to the thin peptidoglycyan walls of *E. coli* (2-3 nm) in comparison to the thickness of peptidoglycyan in *S. auerus* (10 nm) [Kokkoris et al. (2002)]. In our experiments however, Ag-$SiO_2$ powders inhibited the growth of *S. aureus* as well as the growth *E. coli* even the latter has a thicker and more robust cell wall which may hamper the antibacterial activity. As discussed in the introduction section, the antibacterial effect of the Ag-$SiO_2$ powders is induced by the $Ag^+$ adsorption to peptidoglycan in the humid environment. This shows that, the chemical nature of the cell wall seems to be more than its physical properties in controlling its stability against silver biocide.

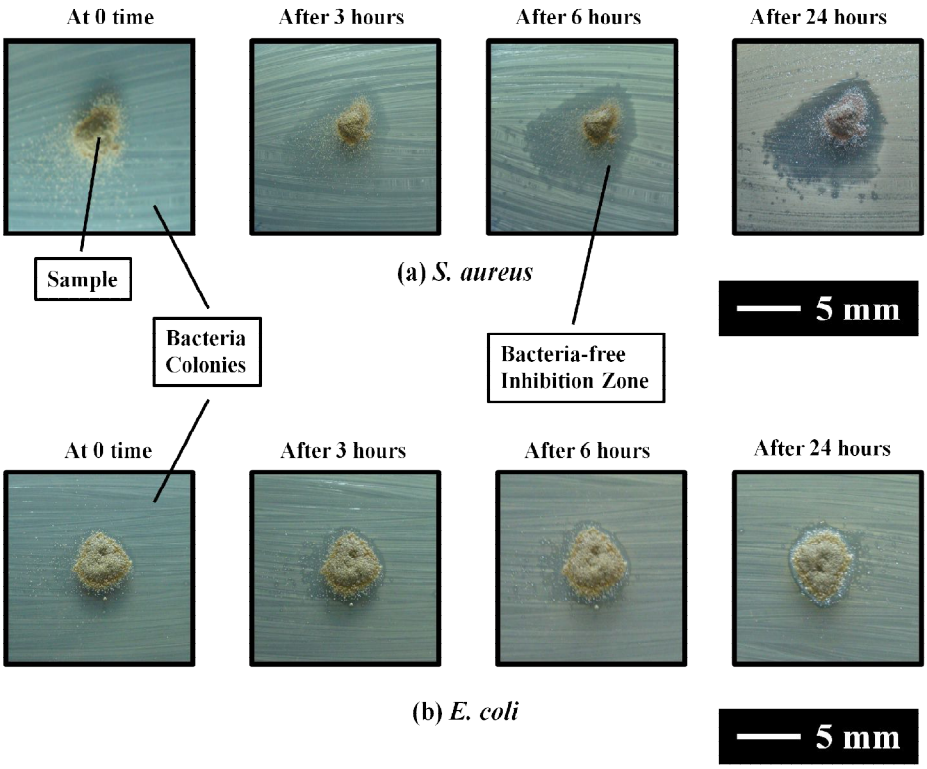


**Figure 3.16** Images of antibacterial test results of sol-gel derived silver-doped silica powders obtained by using indirect synthesis route exposed to low silver dopant concentration of 0.01 M $AgNO_3$ solution and calcined in air at 800°C for 2 h against (a) S. aureus and (b) E. coli after 3,6 and 24 h. The antibacterial activity of the powders at 0 time is shown by the images far left. The white formations are the bacteria colonies. Bacteria-free inhibition zones were present with antibacterial activity. The washing treatment was performed at the same conditions for 6 days.

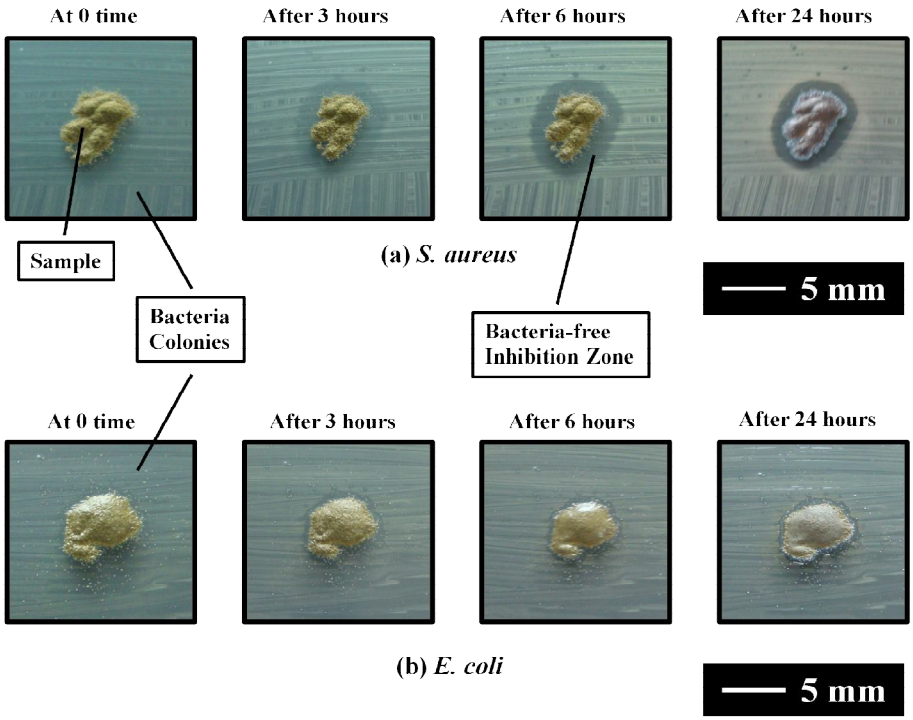


**Figure 3.17** Images of antibacterial test results of sol-gel derived silver-doped silica powders obtained by using indirect synthesis route exposed to high silver dopant concentration of 0.02 M $AgNO_3$ solution and calcined in air at 800°C for 2 h against **(a)** S. aureus and **(b)** E. coli after 3,6 and 24 h. The antibacterial activity of the powders at 0 time is shown by the images far left. The white formations are the bacteria colonies. Bacteria-free inhibition zones were present with antibacterial activity. The washing treatment was performed at the same conditions for 6 days.

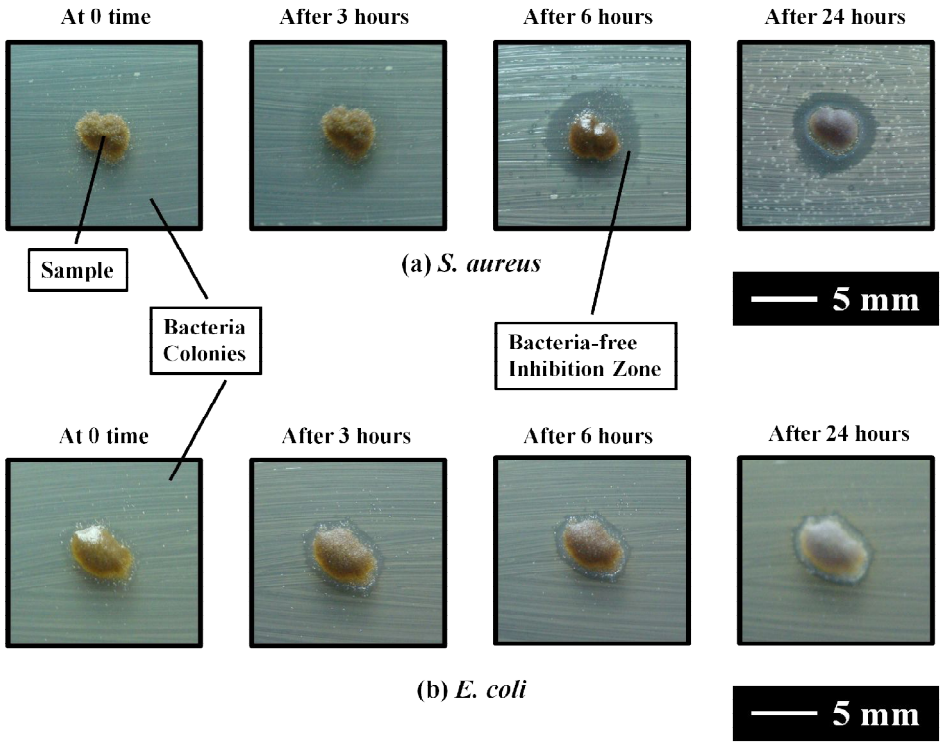


**Figure 3.18** Images of antibacterial test results of sol-gel derived silver-doped silica powders obtained by using direct synthesis route with $[AgNO_3]/[Na_2SiO_3]$=0.004 and calcined in air at 800°C for 2 h aganist **(a)** S. aureus and **(b)** E. coli after 3,6 and 24 h. The antibacterial activity of the powders at 0 time is shown by the images far left. The white formations are the bacteria colonies. Bacteria-free inhibition zones were present with antibacterial activity. The washing treatment was performed at the same conditions for 6 days.

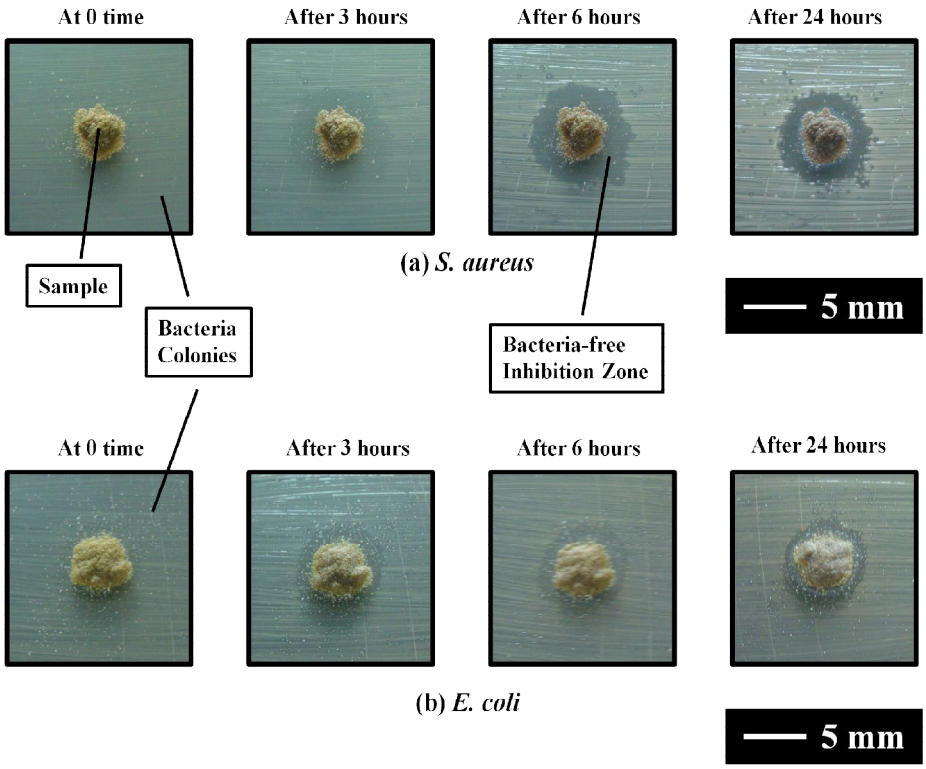


**Figure 3.19** Images of antibacterial test results of sol-gel derived silver-doped silica powders obtained by using direct synthesis route with $[AgNO_3]/[Na_2SiO_3]=0.008$ and calcined in air at 800°C for 2 h against **(a)** S. aureus and **(b)** E. coli after 3,6 and 24 h. The antibacterial activity of the powders at 0 time is shown by the images far left. The white formations are the bacteria colonies. Bacteria-free inhibition zones were present with antibacterial activity. The washing treatment was performed at the same conditions for 6 days.

Figure 3.20 summarizes the antibacterial performance differences for direct and indirect synthesis samples with low and high silver dopant concentration. It is seen that at the samples with low silver amount is more efficient than the samples with high silver amount and as can be understood from the presence of more intense bacteria colonies around the sample free linear features in the case of latter. This phenomenon can be associated with smaller particle size; due better and more effective contact between bacteria and the silver, due higher surface area available in the Ag-$SiO_2$ powders with low silver amount. This was previously described in explaining the possible mechanism for the formation of silver particles upon calcination. Also, it was reported by Kokkoris et al. (2002) that antibacterial activity decreases with an increase in the particle size of silver particles. Furthermore, this figure also reveals that the powders obtained by indirect synthesis route shows better antibacterial performance than the directly synthesized powders. This result was confirmed by XRD results we have shown and can be attributed to the higher extend of silver formation for the indirectly synthesized powders.

Another reason for such differences can be the poor experimental accuracy. In diffusion test the spreading of the powders on the bacteria-containing agar surface might be different due to the powder characteristics, as well due to the surface quality of the agar itself. Unfortunately, these cannot be perfectly standardized due to some practical problems/difficulties. In that respect the interpretation of synthesis method-based differences in bacterial performance should not be considered as an absolutely solid conclusion.

The antibacterial tests however clearly show that the sol-gel derived Ag-$SiO_2$ powders exhibited acceptable antibacterial activity against both *S. aureus* and *E. coli.* Moreover, it can be said that indirectly synthesized powders with low silver dopant showed better antibacterial performance due to presence of silver particles of smaller size. These findings are promising in showing the use of an economically feasible source (water glass) in production of silica particles with controlled antibacterial property.

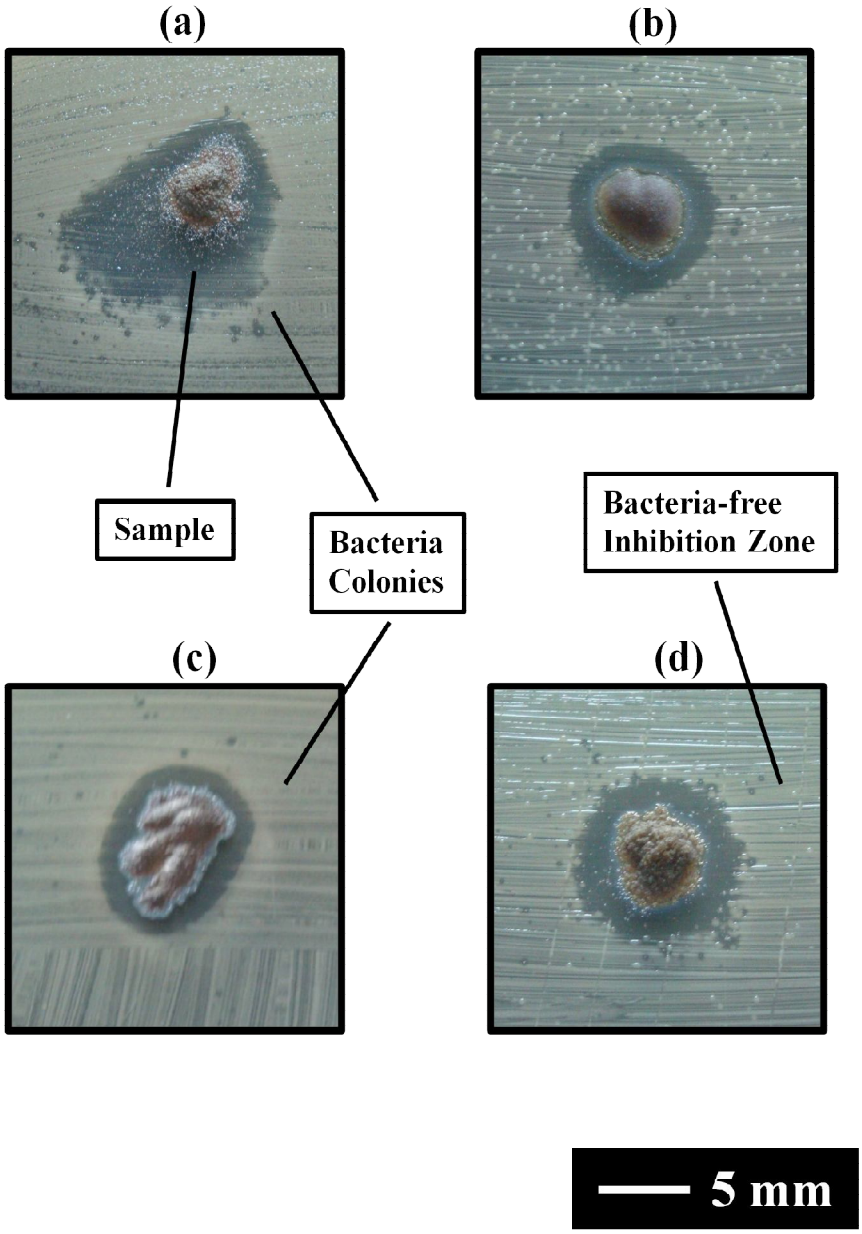


**Figure 3.20** Images of antibacterial test results of sol-gel derived antibacterial silver-doped silica powders heat treated at 800°C after 24 h incubation for **(a)** indirectly synthesized powders exposed to low silver dopant concentration of 0.01 M $AgNO_3$ solution, **(b)** directly synthesized powders with low silver dopant concentration of $[AgNO_3]/[Na_2SiO_3]=0.004$, **(c)** indirectly synthesized powders exposed to high silver dopant concentration of 0.02 M $AgNO_3$ solution and **(d)** directly synthesized powders with high silver dopant concentration of $[AgNO_3]/[Na_2SiO_3]=0.008$.

# CHAPTER 4

# CONCLUSIONS AND FUTURE WORK

## 4.1 Conclusions

In this study, the processing parameters for the silica gel formation from sodium silicate ($Na_2SiO_3$, water glass) was optimized. In addition, sol-gel derived antibacterial silver-doped silica (Ag-$SiO_2$) powders was developed. The general observations and specific findings of the current study are summarized as followings:

### Gelation behavior studies

Silica formation from sodium silicate solution has been investigated with respect to the gelation behavior and time dependent conversion from aqueous to solid (gel) form. Accordingly, gel formation processing parameters for obtaining silica from sodium silicate solution were determined. The specific sol formulation leading to a gel form in an optimum time (at around 1 h) was determined as $Na_2SiO_3$:$H_2O$:catalyst (3 mL:3 mL:20 mL). The gelation occurs at a final pH of 10.50-11.50 when moderately strong catalyst (1.0 M HCl solution) is used.

### Synthesis of antibacterial silver-doped silica (Ag-$SiO_2$) powders

Antibacterial silver-doped silica powders were obtained from sodium silicate by sol-gel method using two different synthesis routes referred as “indirect synthesis” and “direct synthesis”. Powders samples obtained by both synthesis routes were calcined at a range of temperatures (200-800°C) in air for 2 h. However, before heat treatment, obtained gels were washed in order to remove the sodium from the system. Experimental results revealed that sodium was successfully removed from the silica matrix after 6 days of washing treatment. The synthesis method affected both the crystallization of amorphous silica matrix and metallic silver formation together with the antibacterial performance.

Different synthesis routes resulted in two major differences for Ag-$SiO_2$ powders:

i. Powders obtained by indirect synthesis route revealed higher extent of silver particle formation as confirmed by XRD results.

ii. Indirectly synthesized powders samples with low silver dopant amount exhibited better antibacterial performance due to smaller silver particle size in the silica network, providing higher surface area for the intimate contact.

Meanwhile, different silver dopant amount affected the crystallization behavior of the silica network. The crystallization of silica matrix was promoted in the Ag-$SiO_2$ powder samples obtained by indirect synthesis route owing to the smaller silver particle size than that of directly synthesized powders as previously explained by the possible mechanism on metallic silver formation.

The thesis study revealed that silver-doped silica powders obtained from an economically feasible silica source, sodium silicate solution, can be used as a promising antibacterial agent.

### 4.2 Future work

In this study, synthesis of silver-doped silica powders by sol-gel routes and the antibacterial properties of these powders have been demonstrated. The antibacterial performance was mainly related to the synthesis route and the silver amount. It was shown that indirectly synthesized powders with low silver dopant amount revealed better antibacterial performance due to the smaller silver particle size. Meanwhile, silica crystallization was also affected by the silver particle size. Therefore, the microstructural characterization of the synthesized powders should be expanded and SEM/TEM studies can be performed in order to further investigate the effect silver particle size on crystallization of silica and antibacterial performance of the resultant powders..

In addition, the accuracy of antibacterial performance test can be enhanced using pre-shaped “pellet” samples instead of “powder” samples which in turn may provide more systematic and quantitatively comparable results.

Besides, all antibacterial materials should preferentially maintain the bactericidal effect long after its application to surface. Hence, chemical durability test in different pH media can be performed in the future studies in order to get information about the long term durability and performance of these powders.

## REFERENCES


Adams AP, Santschi EM, Mellencamp MA (1999) "Antibacterial properties of a silver chloride-coated nylon wound dressing" Veterinary Surgery 28(4): 219-225.

Akkopru B, Durucan C (2007) "Preparation and microstructure of sol-gel derived silver-doped silica" Journal of Sol-Gel Science and Technology 43(2): 227-236.

Brinker CJ, Scherer GW, Eds. (1990) "Sol-Gel Science: The Physics and Chemistry of Sol-Gel Processing" San Diego: Academic Press.

Chen S, Wu G, Zeng H (2005) "Preparation of high antimicrobial activity thiourea chitosan–Ag+ complex" Carbohydrate Polymers 60(1): 33-38.

Desai NP, Hossainy SFA, Bubbell JA (1992) "Surface-immobilized Polyethyelene Oxide for Bacterial Repellence" Biomaterials 13: 417-420.

De G, Gusso M, Tapfer L, Catalano M, Gonella F, Mattei G, Mazzoldi P, Battaglin G (1996) "Annealing behavior of silver, copper, and silver-copper nanoclusters in a silica matrix synthesized by the sol-gel technique" Journal of Applied Physics 80(12): 6734-6739.

De G, Licciulli A, Massaro C, Tapfer L, Catalano M, Battaglin G, Meneghini C, Mazzoldi P (1996) "Silver nanocrystals in silica by sol-gel processing" Journal of Non-Crystalline Solids 194(3): 225-234.

Feng QL, Wu J, Chen GQ, Cui FZ, Kim TN, Kim JO (2000) "A mechanistic study of the antibacterial effect of silver ions on Escherichia coli and Staphylococcus aureus" Journal of Biomedical Materials Research 52(4): 662-668.

Garnica-Romo MG, González-Hernandez J, Hernández-Landaverde MA, Vorobiev Y, Ruiz F, Martinez JR (2001) "Structure of Heat Treated Sol–Gel SiO2 Glasses Containing Silver" Journal of Material Research 16: 2007-2012.

Garnica-Romo MG, Limón JMY, González-Hernández J, Ramírez-Bon R, Ramírez-Rosales D, Zamorano-Ulloa R, Tirado-Guerra S (2002) "Structure and Electron Spin Resonance of Annealed Sol-Gel Glasses Containing Ag" Journal of Sol-Gel Science and Technology 24(2): 105-112.

Gottardi W, Ed. (1983) "Iodine and Iodine Compunds, Disinfectants, Sterilisation and Preservations" Block S., USA: Lea Febinger.

Grier N, Ed. (1983) "Silver and Its Compounds, Disinfectants, Sterilisation and Preservation" Block S., USA: Lea Febinger

Hilonga A, Kim JK, Sarawade PB, Kim HT (2009) "Reinforced silver-embedded silica matrix from the cheap silica source for the controlled release of silver ions" Applied Surface Science 255(19): 8239-8245.

Hilonga A, Kim JK, Sarawade PB, Kim HT (2010) "Influence of annealing conditions on the properties of reinforced silver-embedded silica matrix from the cheap silica source" Applied Surface Science 256(9): 2849-2855.

Jeon H-J, Yi S-C, Oh S-G (2003) "Preparation and antibacterial effects of Ag–SiO2 thin films by sol–gel method" Biomaterials 24(27): 4921-4928.

Kawashita M, Tsuneyama S, Miyaji F, Kokubo T, Kozuka H, Yamamoto K (2000) "Antibacterial silver-containing silica glass prepared by sol–gel method" Biomaterials 21(4): 393-398.

Kawashita M, Toda S, Kim H-M, Kokubo T, Masuda N (2003) "Preparation of antibacterial silver-doped silica glass microspheres" Journal of Biomedical Materials Research Part A 66A(2): 266-274.

Kokkoris M, Trapalis CC, Kossionides S, Vlastou R, Nsouli B, Grötzschel R, Spartalis S, Kordas G, Paradellis Th (2002) "RBS and HIRBS studies of nanostructured AgSiO2 sol–gel thin coatings" Nuclear Instruments and Methods in Physics Research Section B: Beam Interactions with Materials and Atoms 188(1–4): 67-72.

Kurosaka N, Nihei T, Kumada H, Umemoto T, Kondo Y, Yoshino N, Teranaka T (2000) "Poly(fluoro)triisocyanatosilane Surface Modification Reduces Streptococcus Mutans Adherence" Journal of Dental Research 79(465).

Mennig M, Spanhel J, Schmidt H, Betzholz S (1992) "Photoinduced formation of silver colloids in a borosilicate sol-gel system" Journal of Non-Crystalline Solids 147–148(0): 326-330.

Mennig M, Schmitt M, Schmidt H (1997) "Synthesis of Ag-colloids in sol-gel derived SiO2-coatings on glass" Journal of Sol-Gel Science and Technology 8(1): 1035-1042.

Nishino A, Tomioka T, Tomita K, Kobayashi S , Eds. (1996) "Science of Antibacterial Materials" Tokyo: Advisory Committee for Industry Press.

Ohko Y, Utsumi Y, Niwa C, Tatsuma T, Kobayakawa K, Satoh Y, Kubota Y, Fujishima A (2001) "Self-sterilizing and self-cleaning of silicone catheters coated with TiO2 photocatalyst thin films: A preclinical work" Journal of Biomedical Materials Research 58(1): 97-101.

Ohtani A, Ed. (1997) "Various Antibacterial Inorganic Materials and Their High Applicable Technology" Tokyo: IPC Press.

Ortega-Zarzosa G, Martínez JR, Robledo-Cabrera A, Martínez-Castañón GA, Sánchez-Loredo MG, Ruiz F (2003) "Annealing Behavior of Silica Gel Powders Modified with Silver Crystalline Aggregates" Journal of Sol-Gel Science and Technology 27(3): 255-262.

Page K, Palgrave RG, Parkin IP, Wilson M, Savin SLP, Chadwick AV (2007) "Titania and silver-titania composite films on glass-potent antimicrobial coatings" Journal of Materials Chemistry 17(1): 95-104.

Pai MP, Pendland SL, Danziger LH (2001) "Antimicrobial-coated/bonded and -impregnated intravascular catheters" The Annals of Pharmacotherapy 35(10): 1255-1263.

Renteria VM, Campero A, Garcia MJ (1998) "Thermochromic Properties of Silver Colloids Embedded in SiO2 Gels" Journal of Sol-Gel Science and Technology 13(1): 663-666.

Ritzer B, Villegas M, Fernández Navarro J (1997) "Influence of temperature and time on the stability of silver in silica sol-gel glasses" Journal of Sol-Gel Science and Technology 8(1): 917-921.

Sakka S and H Kozuka (1998) "Sol-Gel Preparation of Coating Films Containing Noble Metal Colloids" Journal of Sol-Gel Science and Technology 13(1): 701-705.

Serezhkina SV, Potapenko LT, Bokshits YV, Shevchenko GP, Sviridov VV (2003) "Preparation of Silver Nanoparticles in Oxide Matrices Derived by the Sol–Gel Method" Glass Physics and Chemistry 29(5): 484-489.

Tiller JC, Liao C-J, Lewis K, Klibanov AM (2001) "Designing surfaces that kill bacteria on contact" Proceedings of the National Academy of Sciences 98(11): 5981-5985.

Tiller JC, Hartmann L, Scherble J (2005) "Reloadable antimicrobial coatings based on amphiphilic silicone networks" Surface Coatings International Part B: Coatings Transactions 88(1): 49-53.

Weiping C and Z Lide (1996) "Characterization and the optical switching phenomenon of porous silica dispersed with silver nano-particles within its pores" Journal of Physics: Condensed Matter 8(40): L591.

Wu PW, Dunn B, Doan V, Schwartz BJ, Yablonovitch E, Yamane M (2000) "Controlling the Spontaneous Precipitation of Silver Nanoparticles in Sol-Gel Materials" Journal of Sol-Gel Science and Technology 19: 249- 252.

Xing Y, Yang X, Dai J (2007) "Antimicrobial finishing of cotton textile based on water glass by sol–gel method" Journal of Sol-Gel Science and Technology 43(2): 187-192.

Yoshinari T and M Uchida (1993) "Antimicrobial ceramics" Ceramics 28: 651–657

Zayat M, Einot D, Reisfeld R (1997) "In-Situ Formation of AgCl Nanocrystallites in Films Prepared by the Sol-Gel and Silver Nanoparticles in Silica Glass Films" Journal of Sol-Gel Science and Technology 10(1): 67-74.